
ESTIMATING KNOTS IN BILINEAR SPLINE GROWTH MODELS WITH TIME-INVARIANT COVARIATES IN THE FRAMEWORK OF INDIVIDUAL MEASUREMENT OCCASIONS

A PREPRINT

Jin Liu
Department of Biostatistics
Virginia Commonwealth University
Veronica.Liu0206@gmail.com

Le Kang
Department of Biostatistics
Virginia Commonwealth University

Robert M. Kirkpatrick
Department of Psychiatry
Virginia Commonwealth University

Roy T. Sabo
Department of Biostatistics
Virginia Commonwealth University

Robert A. Perera*
Department of Biostatistics
Virginia Commonwealth University

June 17, 2022

ABSTRACT

The linear spline growth model (LSGM) is a popular tool for examining nonlinear change patterns over time. It approximates complex patterns by attaching at least two linear trajectories. Besides examining within-person changes and between-person differences of trajectories simultaneously, it poses interesting statistical challenges, such as estimating the location of a change point (or knot), the knot's variance, prediction of the knot location using covariates, and analyzing data with individually-varying times points (ITPs). We developed a pair of bilinear spline growth models with time-invariant covariates (BLSGMs-TICs) to estimate a knot and its variability as well as to investigate predictors of individual trajectories in the ITPs framework. We present the proposed methods by simulation studies and a real-world data analysis. Our simulation studies demonstrate that the proposed BLSGMs-TICs generally estimate the parameters of interest unbiasedly, precisely and exhibit appropriate confidence interval coverage. An empirical example using longitudinal mathematics scores shows that the model can estimate the knot and its variance as well as identify predictors to explain the knot variability. We also provide the corresponding code for the proposed models.

Keywords Linear spline growth models · Unknown knots · Individually-varying time points · Time-invariant covariates · Simulation studies

1 Introduction

Longitudinal studies of change are popular in various disciplines to evaluate individual growth over time. If a process under investigation is followed for a long enough time duration, it is likely to exhibit some degree of nonlinear change in which the curve has a nonconstant relationship to recorded time. Nonlinear change patterns exist in multiple areas, for example, verbal ability (Jones and Bayley, 1941), mathematical ability (Harring, 2009), cognitive accelerated aging (Finkel et al., 2003), and rehabilitation after the total knee arthroplasty (Riddle et al., 2015; Dumenci et al., 2019). When analyzing such trajectories, it is of interest to investigate within-individual change and between-individual differences simultaneously. One approach to examining the mean change pattern and the individual variability around it is the linear spline growth model (LSGM) (Grimm et al., 2016), also referred to as a piecewise linear latent growth model (Kohli, 2011; Kohli et al., 2013; Kohli and Harring, 2013; Sterba, 2014). By attaching at least two linear pieces (see Figure 1), the linear spline (or piecewise linear) functional form can approximate more complex underlying change

*CONTACT Robert A. Perera. Email: robert.perera@vcuhealth.org

patterns. Previous studies have demonstrated a broad application of linear spline trajectory. It has been employed to assess post-surgical rehabilitation (Riddle et al., 2015; Dumenci et al., 2019), the learning process of a specific task (Cudeck and Klebe, 2002), the onset of alcohol abuse (Li et al., 2001) and intellectual development (Marcoulides, 2018). The LSGM can be modeled either in the structural equation modeling (SEM) framework or using a mixed-effects model (Grimm et al., 2016). This article focuses on the LSGM in the SEM framework.

Under assumptions that between-individual differences in growth factors (i.e., individuals' intercepts and slopes) follow a multivariate normal distribution and that all individuals belong to one single population (Bollen and Curran, 2005), researchers employed the LSGM to investigate a nonlinear change of an individual over time as well as the difference across such individuals' changes through estimating the mean vector and the variance-covariance matrix of such growth factors. When estimating, the LSGM poses several interesting statistical challenges. First, besides growth factors, such as intercepts and slopes, it is of interest to examine the characteristics of the inflection point or 'knot' at which two segments join together. When fitting LSGMs, knots can be either pre-specified by a theory-driven method (Flora, 2008; Sterba, 2014; Riddle et al., 2015; Dumenci et al., 2019) or be detected automatically via model selection based on information criteria like BIC (Marcoulides, 2018), or be viewed as a parameter in a more flexible setting (Kwok et al., 2010; Kohli, 2011; Kohli et al., 2013; Kohli and Harring, 2013; Kohli et al., 2015a,b).

The most intuitive but useful linear spline function is a bilinear spline growth model (BLSGM, or linear-linear piecewise model). Not only can this functional form identify a process that is theoretically to be two stages with different rates of change (Riddle et al., 2015; Dumenci et al., 2019), but it also can help to approximate other nonlinear change patterns (Kohli et al., 2015a). Harring et al. (2006) developed a BLSGM with an unknown fixed knot with a unified functional form of two linear pieces through reparameterization, which is realized by re-expressing growth factors as linear combinations of their original form. Kohli (2011), Kohli et al. (2013) and Grimm et al. (2016) provided the transformation matrices that allow the reparameterized mean vector and variance-covariance matrix to be transformed back to the original parameterization so estimates are interpretable. By implementing this model, Kohli et al. (2013) examined the development in each stage and estimated a fixed knot for procedural learning task research. In addition, Preacher and Hancock extended the model with an unknown fixed knot to estimate the variance of the knot simultaneously, in which the knot was viewed as an additional growth factor besides the intercept and two slopes (Preacher and Hancock, 2015).

Although such developed reparameterized BLSGMs with an unknown knot make it possible to estimate the inflection point as well as its variance conveniently, they may be less useful when being employed to analyze the piecewise change patterns. First, the reparameterized procedure provided by Harring et al. (2006), Kohli (2011), and Kohli et al. (2013) does not provide the same notation and expression of reparameterized growth factors for the two situations shown in Figure 1 (i.e., the first slope is greater or less than the second slope). In this work, by extending the study of Tishler and Zang (1981) and Seber and Wild (2003) to the BLSGM framework, we unified the reparameterization procedure and then (inverse-)transformation matrices between the original and the reparameterized growth factors.

Second, to our knowledge, no existing studies provide transformation and inverse-transformation matrices of growth factors in the original and reparameterized settings for the BLSGM to estimate a knot with its variance, though such matrices have been presented for the BLSGM with an unknown fixed knot (Kohli, 2011; Kohli et al., 2013; Grimm et al., 2016). The parameters of greatest interest from such models are the knot and its variance. However, the characteristics of other growth factors, such as the initial status and the rate of the change of each stage, even those of the associations between such growth factors also provide information that helps to capture features of trajectories.

More importantly, the BLSGM with an unknown knot allows inferences for the mean of such nonlinear change patterns for a single group as well as the variability in individual trajectories around the mean change. Additionally, it is of interest to explore time-invariant covariates (also referred to as 'individual-level covariates') that are associated with the between-individual differences in the trajectories. The existing frameworks do not incorporate individual-level covariates, which prohibits investigation of predictors to explain the variances of the knot and other growth factors. It should be noted that the time-invariant covariates in the BLSGM explain the variability of each reparameterized growth factor. To investigate the association between the growth factors and the covariates in the original setting, (inverse-)transformation matrices for the effects of the covariates are needed. Lastly, to our knowledge, no previous studies provided a full set of recommendations for applied practice on whether we need to consider the variability of the inflection point or possible following steps after estimating the variance. In this article, we provide recommendations for practice by presenting how to apply the proposed method to a real-world data set.

Another statistical challenge of longitudinal data sets is the individual-varying measurement occasion (Cook and Ware, 1983; Mehta and West, 2000; Finkel et al., 2003). This can occur when time is measured precisely (e.g., exact date and time of measurement), or if responses are self-initiated or randomly assigned. For instance, in an adolescent smoking study, participants were asked to complete a questionnaire on pocket computers immediately after smoking (Hedeker et al., 2006). One possible way to fit growth models with individual measurement occasions is the definition

variable approach, in which the ‘definition variables’ are defined as observed variables that are employed to adjust model parameters to individual-specific values (Mehta and West, 2000; Mehta and Neale, 2005). In our case, these individual-specific values are individual measurement occasions.

In the SEM framework, demonstrations of how to incorporate the definition variable approach have concerned either linear trajectories (Mehta and West, 2000) or BLSGM with a pre-specified inflection point (Sterba, 2014). However, to our knowledge, no previous studies have demonstrated how to implement BLSGMs with an unknown knot with exactly individually varying measurement time in the SEM framework, although this extension has been recommended (Grimm et al., 2016).

The proposed model fills an existing gap by describing how to fit a BLSGM with time-invariant covariates (BLSGM-TICs) in the individually-varying time points (ITPs) framework to estimate an inflection time point with its variance and other growth factors as well as to explore predictors of between-individual differences in trajectories. In the current work, we have three major aims. First, we aim to capture characteristics of individual trajectories with bilinear spline functional form and identify covariates that help explain the individual difference in trajectories. More importantly, we desire to make the statistical inference of the intercept, two slopes and the knot. Second, we want to fit the model with individually varying time scores due to its ubiquity in longitudinal studies. Third, we provide a set of recommendations for real-world practice. To realize this aim, we also develop a BLSGM-TICs for estimating an inflection point without variability.

The remainder of this article is organized as follows. In the method section, we first present the model specification of the BLSGM-TICs to estimate an inflection point and its variance. Next, we introduce how to reparameterize growth factors and the corresponding path coefficients from the TICs to the growth factors to make them estimable in the SEM framework and how to transform them back after estimation for interpretation purposes. We then propose one possible reduced BLSGM-TICs to estimate the knot without variance. We next describe the model estimation as well as the Monte Carlo simulation design for model evaluation. In the section of simulation result, we present the evaluation of the model performance concerning the non-convergent rate, the proportion of improper solutions, as well as the bias, the root-mean-squared-error (RMSE) and the empirical coverage for a nominal 95% confidence interval of each parameter of interest. In the next section, by applying the proposed BLSGM-TICs to a data set of repeated measures of mathematics scores from the Early Childhood Longitudinal Study, Kindergarten Class of 2010 – 11 (ECLS-K: 2011), we give a set of feasible recommendations for real-world practice. Finally, discussions are framed concerning the model’s limitations as well as future directions.

2 Method

2.1 Model Specification

With an assumption that all subjects are from a single population conditional on individual-level covariates, the BLSGM-TICs with an unknown knot is given by

$$\mathbf{y}_i = \mathbf{\Lambda}_i(\gamma_i)\eta_i + \epsilon_i, \quad (1)$$

where \mathbf{y}_i is a $J \times 1$ vector of the repeated outcomes for the i^{th} person (in which J is the number of measurements), $\mathbf{\Lambda}_i(\gamma_i)$, which is a function of its unknown knot γ_i , is a $J \times 3$ matrix of factor loadings determined by definition variables, ϵ_i is a $J \times 1$ vector of residuals for the i^{th} person, and η_i is a 3×1 vector of growth factors ($\eta_i = (\eta_{0i}, \eta_{1i}, \eta_{2i})^T$, for an intercept and two slopes) of the i^{th} individual. η_i can be regressed on individual-level covariates,

$$\eta_i = \alpha + \mathbf{B}\mathbf{X}_i + \zeta_i \quad (2)$$

where α is a 3×1 vector of growth factor intercepts (which is the mean vector of growth factors if the TICs are centered), \mathbf{B} is a $3 \times c$ matrix of regression coefficients (in which c is the number of TICs) from TICs to growth factors, \mathbf{X}_i , which may either be continuous or be binary, is a $c \times 1$ vector of covariates of the i^{th} individual, and ζ_i is a 3×1 vector of deviations of the i^{th} subject from the factor means.

Tishler and Zang (1981) and Seber and Wild (2003) showed that the bilinear spline regression model can be written as either the minimum or maximum response value of two trajectories. By extending such expressions to the BLSGM framework, two forms of bilinear spline for the i^{th} individual are shown in Figure 1. In the left panel ($\eta_{1i} > \eta_{2i}$), the measurement y_{ij} should always be the minimum value of two lines; that is, $y_{ij} = \min(\eta_{0i} + \eta_{1i}t_{ij}, \eta_{02i} + \eta_{2i}t_{ij})$. To

unify the expression of measurements pre- and post-knot, we have the following equation

$$\begin{aligned}
y_{ij} &= \min(\eta_{0i} + \eta_{1i}t_{ij}, \eta_{02i} + \eta_{2i}t_{ij}) \\
&= \frac{1}{2}(\eta_{0i} + \eta_{1i}t_{ij} + \eta_{02i} + \eta_{2i}t_{ij} - |\eta_{0i} + \eta_{1i}t_{ij} - \eta_{02i} - \eta_{2i}t_{ij}|) \\
&= \frac{1}{2}(\eta_{0i} + \eta_{1i}t_{ij} + \eta_{02i} + \eta_{2i}t_{ij}) - \frac{1}{2}(|\eta_{0i} + \eta_{1i}t_{ij} - \eta_{02i} - \eta_{2i}t_{ij}|) \\
&= \frac{1}{2}(\eta_{0i} + \eta_{02i} + \eta_{1i}t_{ij} + \eta_{2i}t_{ij}) - \frac{1}{2}(\eta_{1i} - \eta_{2i})|t_{ij} - \gamma_i| \\
&= \eta'_{0i} + \eta'_{1i}(t_{ij} - \gamma_i) + \eta'_{2i}|t_{ij} - \gamma_i| \\
&= \eta'_{0i} + \eta'_{1i}(t_{ij} - \gamma_i) + \eta'_{2i}\sqrt{(t_{ij} - \gamma_i)^2},
\end{aligned} \tag{3}$$

where η'_{0i} , η'_{1i} and η'_{2i} are the measurement at the knot, the mean of two slopes, and the half difference between two slopes. Through straightforward algebra, the measurement y_{ij} of the bilinear spline in the right panel, in which the measurement y_{ij} should always be the maximum value of two lines, has the identical final form as Equation (3).

=====
Insert Figure 1 about here
=====

In the model shown in Equation (1), the inflection point γ_i , like the intercept and two slopes, varies across individuals and then is viewed as an additional growth factor. SEM models fail to estimate it directly (Grimm et al., 2016), due to the nonlinear relationship between the repeated outcome and the growth factors. The proposed model can be expressed as a linear combination of all four growth factors through the Taylor series expansion (Browne and du Toit, 1991; Grimm et al., 2016). By this approach (see Appendix A.1 for detailed derivation), we obtain the reparameterized growth factors and the corresponding factor loadings for the i^{th} individual, which can be expressed as

$$\eta'_i = \begin{pmatrix} \eta'_{0i} & \eta'_{1i} & \eta'_{2i} & \delta_i \end{pmatrix}^T = \begin{pmatrix} \eta_{0i} + \gamma_i\eta_{1i} & \frac{\eta_{1i} + \eta_{2i}}{2} & \frac{\eta_{2i} - \eta_{1i}}{2} & \gamma_i - \mu_\gamma \end{pmatrix}^T \tag{4}$$

and

$$\Lambda'_i(\gamma_i) = \begin{pmatrix} 1 & t_{ij} - \mu_\gamma & |t_{ij} - \mu_\gamma| & -\mu_{\eta'_2} - \frac{\mu'_{\eta'_2}(t_{ij} - \mu_\gamma)}{|t_{ij} - \mu_\gamma|} \end{pmatrix} \quad (j = 1, \dots, J), \tag{5}$$

respectively, where μ_γ is the knot mean and δ_i is the deviation from the knot mean of the i^{th} individual. With η'_i and $\Lambda'_i(\gamma_i)$ as shown in Equations (4) and (5), we then respecify the BLSGM-TICs in Equations (1) and (2) as Equations

$$\mathbf{y}_i = \Lambda'_i(\gamma_i)\eta'_i + \epsilon_i \tag{6}$$

and

$$\eta'_i = \alpha' + \mathbf{B}'\mathbf{X}_i + \zeta'_i, \tag{7}$$

respectively, where α' is a 4×1 vector of reparameterized growth factor intercepts while \mathbf{B}' is a $4 \times c$ matrix of reparameterized path coefficients (in which c is the number of TICs) from TICs to the growth factors, and ζ'_i is a 4×1 vector of normally distributed deviations of the i^{th} individual from the reparameterized growth factor means. Such growth factor intercepts and coefficients also needed to be transformed back to be interpretable as the relationship between the growth factors in the original setting.

2.2 Transformation Matrix and Inverse-transformation Matrix

When fitting a model in the SEM framework, especially a complex model, it is helpful to select a proper set of initial values to improve the likelihood of convergence and accelerate the computational process. Generally, descriptive statistics and visualization are tools for researchers to decide suitable initial values for the parameters of interest. However, it may not be straightforward for the reparameterized parameters. Accordingly, the transformation matrices from parameters in the original frame to those in the reparameterized setting help decide appropriate initial values. More importantly, all re-expressed parameters need to be transformed back to be interpretable after estimating, which can be realized by inverse-transformation matrices. With straightforward algebra, we obtain the transformation and inverse-transformation matrices for the mean vectors and the variance-covariance matrices.

For the i^{th} individual, as shown in Equation (4), the relationships between the original growth factors (η_i) and the reparameterized growth factors (η'_i) are \mathbf{G}_i and \mathbf{G}_i^{-1} are given by

$$\begin{aligned}\eta'_i &= (\eta'_{0i} \ \eta'_{1i} \ \eta'_{2i} \ \delta_i)^T = (\eta_{0i} + \gamma_i \eta_{1i} \ \frac{\eta_{1i} + \eta_{2i}}{2} \ \frac{\eta_{2i} - \eta_{1i}}{2} \ \gamma_i - \mu_\gamma)^T \\ &= \begin{pmatrix} 1 & \gamma_i & 0 & 0 \\ 0 & 0.5 & 0.5 & 0 \\ 0 & -0.5 & 0.5 & 0 \\ 0 & 0 & 0 & 1 \end{pmatrix} \begin{pmatrix} \eta_{0i} \\ \eta_{1i} \\ \eta_{2i} \\ \gamma_i - \mu_\gamma \end{pmatrix} = \mathbf{G}_i \times \begin{pmatrix} \eta_{0i} \\ \eta_{1i} \\ \eta_{2i} \\ \gamma_i - \mu_\gamma \end{pmatrix}\end{aligned}$$

and

$$\begin{aligned}\eta_i &= (\eta_{0i} \ \eta_{1i} \ \eta_{2i} \ \gamma_i)^T = (\eta'_{0i} - \gamma_i \eta'_{1i} + \gamma_i \eta'_{2i} \ \eta'_{1i} - \eta'_{2i} \ \eta'_{1i} + \eta'_{2i} \ \delta_i + \mu_\gamma)^T \\ &= \begin{pmatrix} 1 & -\gamma_i & \gamma_i & 0 \\ 0 & 1 & -1 & 0 \\ 0 & 1 & 1 & 0 \\ 0 & 0 & 0 & 1 \end{pmatrix} \begin{pmatrix} \eta'_{0i} \\ \eta'_{1i} \\ \eta'_{2i} \\ \delta_i + \mu_\gamma \end{pmatrix} = \mathbf{G}_i^{-1} \times \begin{pmatrix} \eta'_{0i} \\ \eta'_{1i} \\ \eta'_{2i} \\ \delta_i + \mu_\gamma \end{pmatrix}.\end{aligned}$$

It is noted that the (inverse-) transformation matrix is individual-level due to the knot variance. For implementation, we employ the population-level (inverse-) transformation matrix to simplify the calculation. In Appendix A.2, we present the conditions under which the individual-level matrices can be approximated to be the population-level ones.

The transformation matrix and the inverse-transformation matrix between the mean vector of the original growth factors (μ_η) and that of the reparameterized growth factors ($\mu_{\eta'}$) are

$$\mu_{\eta'} \approx \begin{pmatrix} 1 & \mu_\gamma & 0 & 0 \\ 0 & 0.5 & 0.5 & 0 \\ 0 & -0.5 & 0.5 & 0 \\ 0 & 0 & 0 & 1 \end{pmatrix} \times \begin{pmatrix} \mu_{\eta_0} \\ \mu_{\eta_1} \\ \mu_{\eta_2} \\ 0 \end{pmatrix} = \mathbf{G} \times \begin{pmatrix} \mu_{\eta_0} \\ \mu_{\eta_1} \\ \mu_{\eta_2} \\ 0 \end{pmatrix}$$

and

$$\mu_\eta \approx \begin{pmatrix} 1 & -\mu_\gamma & \mu_\gamma & 0 \\ 0 & 1 & -1 & 0 \\ 0 & 1 & 1 & 0 \\ 0 & 0 & 0 & 1 \end{pmatrix} \times \begin{pmatrix} \mu_{\eta'_0} \\ \mu_{\eta'_1} \\ \mu_{\eta'_2} \\ \mu_\gamma \end{pmatrix} = \mathbf{G}^{-1} \times \begin{pmatrix} \mu_{\eta'_0} \\ \mu_{\eta'_1} \\ \mu_{\eta'_2} \\ \mu_\gamma \end{pmatrix};$$

and those between the variance-covariance matrix of the original growth factors (Ψ_η) and that of the reparameterized growth factors ($\Psi_{\eta'}$) are

$$\begin{aligned}\Psi_{\eta'} &\approx E(\text{Var}(\mathbf{G}_i \times \eta_i | \gamma_i)) = \mathbf{E}(\nabla \mathbf{G}_i \text{Var}(\eta_i) \nabla \mathbf{G}_i^T) \\ &\approx \begin{pmatrix} 1 & \mu_\gamma & 0 & \mu_{\eta_1} \\ 0 & 0.5 & 0.5 & 0 \\ 0 & -0.5 & 0.5 & 0 \\ 0 & 0 & 0 & 1 \end{pmatrix} \Psi_\eta \begin{pmatrix} 1 & \mu_\gamma & 0 & \mu_{\eta_1} \\ 0 & 0.5 & 0.5 & 0 \\ 0 & -0.5 & 0.5 & 0 \\ 0 & 0 & 0 & 1 \end{pmatrix}^T \\ &= \nabla \mathbf{G} \Psi_\eta \nabla \mathbf{G}^T\end{aligned}$$

and

$$\begin{aligned}\Psi_\eta &\approx E(\text{Var}(\mathbf{G}_i^{-1} \times \eta'_i | \gamma_i)) = \mathbf{E}(\nabla \mathbf{G}_i^{-1} \text{Var}(\eta'_i) \nabla \mathbf{G}_i^{-1T}) \\ &\approx \begin{pmatrix} 1 & -\mu_\gamma & \mu_\gamma & 0 \\ 0 & 1 & -1 & 0 \\ 0 & 1 & 1 & 0 \\ 0 & 0 & 0 & 1 \end{pmatrix} \Psi_{\eta'} \begin{pmatrix} 1 & -\mu_\gamma & \mu_\gamma & 0 \\ 0 & 1 & -1 & 0 \\ 0 & 1 & 1 & 0 \\ 0 & 0 & 0 & 1 \end{pmatrix}^T \\ &= \nabla \mathbf{G}^{-1} \Psi_{\eta'} \nabla \mathbf{G}^{-1T}.\end{aligned}$$

When fitting the BLSGM-TICs using software such as the *R* package *OpenMx*, which allows for matrix calculation, we only need to provide the matrices \mathbf{G} , \mathbf{G}^{-1} , $\nabla \mathbf{G}$ and $\nabla \mathbf{G}^{-1}$ for transformation between the original setting and the reparameterized frame. In contrast, when (inversely) transforming parameters using SEM software that does not allow matrix algebra like *Mplus*, we need to give an expression of each cell of the mean vectors and the variance-covariance matrices, all of which are provided in Appendix A.3.

When regressing growth factors on the individual-level covariates as we did in Equation (2), we also need to re-express the path coefficients if we reparameterize the growth factors. By centering the covariates, on the one hand, we make the vector α equivalent to the mean vector of growth factor. Accordingly, the transformation and inverse-transformation matrices between the original intercepts (α) and the reparameterized intercepts (α') are \mathbf{G} and \mathbf{G}^{-1} , respectively. On the other hand, through centering the covariates, we simplify the transformation and inverse-transformation matrices between the original path coefficients (\mathbf{B}) and the reparameterized path coefficients (\mathbf{B}') as $\nabla\mathbf{G}$ and $\nabla\mathbf{G}^{-1}$, respectively. The detailed derivation is shown in Appendix A.4.

2.3 Model Estimation

To simplify estimation, we assume that the growth factors (the intercept, two slopes and the knot) are normally distributed conditional on individual-level covariates and that individual residuals follow identical and independent normal distributions over time, that is, $\epsilon_i \sim \mathbf{N}(\mathbf{0}, \theta_\epsilon \mathbf{I})$. Then for the i^{th} individual, the expected mean vector and the variance-covariance structure of the repeated measurements of the model given in Equations (6) and (7) can be expressed as²

$$\mu_i = \Lambda'_i(\gamma_i)(\alpha' + \mathbf{B}'\mu_{\mathbf{X}}) \quad (8)$$

and

$$\Sigma_i = \Lambda'_i(\gamma_i)\Psi_{\eta'}\Lambda'_i(\gamma_i)^{\mathbf{T}} + \Lambda'_i(\gamma_i)\mathbf{B}'\Phi\mathbf{B}'^{\mathbf{T}}\Lambda'_i(\gamma_i)^{\mathbf{T}} + \theta_\epsilon\mathbf{I}, \quad (9)$$

where $\mu_{\mathbf{X}}$ and Φ are the mean vector ($c \times 1$) and the variance-covariance matrix ($c \times c$) of the TICs, respectively, other parameters have the exactly same definition in Equations (6) and (7).

The parameters in the model given in Equations (6) and (7) include the mean vector and the variance-covariance matrix of reparameterized growth factors, the re-expressed path coefficients as well as the means and the variance-covariance structure of subject-level covariates. Then by the inverse-transformation matrices provided in Section 2.2, the parameters in the original setting can be calculated. Θ_1 and Θ'_1 in Equations

$$\begin{aligned} \Theta_1 &= \{\alpha, \Psi_{\eta}, \mathbf{B}, \mu_{\mathbf{X}}, \Phi, \theta_\epsilon\} \\ &= \{\mu_{\eta_0}, \mu_{\eta_1}, \mu_{\eta_2}, \mu_{\gamma}, \psi_{00}, \psi_{01}, \psi_{02}, \psi_{0\gamma}, \psi_{11}, \psi_{12}, \psi_{1\gamma}, \psi_{22}, \psi_{2\gamma}, \psi_{\gamma\gamma}, \mathbf{B}, \mu_{\mathbf{X}}, \Phi, \theta_\epsilon\} \end{aligned} \quad (10)$$

and

$$\begin{aligned} \Theta'_1 &= \{\alpha', \Psi_{\eta'}, \mathbf{B}', \mu_{\mathbf{X}}, \Phi, \theta_\epsilon\} \\ &= \{\mu'_{\eta_0}, \mu'_{\eta_1}, \mu'_{\eta_2}, \mu_{\gamma}, \psi'_{00}, \psi'_{01}, \psi'_{02}, \psi'_{0\gamma}, \psi'_{11}, \psi'_{12}, \psi'_{1\gamma}, \psi'_{22}, \psi'_{2\gamma}, \psi_{\gamma\gamma}, \mathbf{B}', \mu_{\mathbf{X}}, \Phi, \theta_\epsilon\} \end{aligned} \quad (11)$$

list the parameters in the original and the reparameterized frames, respectively.

We then use full information maximum likelihood (FIML) to estimate Θ'_1 due to the potential heterogeneity of individual contributions to the likelihood. The log-likelihood function of each individual and that of the overall sample can be expressed as

$$\log \text{lik}_i(\Theta'_1 | \mathbf{y}_i) = C - \frac{1}{2} \ln |\Sigma_i| - \frac{1}{2} (\mathbf{y}_i - \mu_i)^{\mathbf{T}} \Sigma_i^{-1} (\mathbf{y}_i - \mu_i), \quad (12)$$

and

$$\log \text{lik}(\Theta'_1 | \mathbf{y}) = \sum_{i=1}^n \log \text{lik}_i(\Theta'_1 | \mathbf{y}_i), \quad (13)$$

respectively, where C is a constant, n is the number of individuals, μ_i and Σ_i are the mean vector and the variance-covariance matrix of \mathbf{y}_i , which have been defined in Equations (8) and (9), respectively. We construct the proposed BLSGM-TICs using the R package *OpenMx* with the optimizer CSOLNP (Neale et al., 2016; Pritikin et al., 2015; Hunter, 2018; Boker et al., 2018), with which we are able to fit the proposed model and implement the transformation matrix as well as inverse-transformation matrix as shown in Section 2.2 efficiently.

2.4 Reduced Model

By fixing the between-individual differences in the inflection point to 0, the model in Equation (1) has a reduced form for estimating an unknown knot without considering variability given by

$$\mathbf{y}_i = \Lambda_i(\gamma)\eta_i + \epsilon_i, \quad (14)$$

²We extend the expressions of the expected mean vector and variance-covariance structure of repeated measurements in a study of Grimm, Ram, and Estabrook (Grimm et al., 2016) to the framework of our model.

where $\Lambda_i(\gamma)$, which is a function of a fixed inflection point γ , is a $J \times 3$ matrix of factor loadings.

When being modeled in the SEM framework, this reduced model still needs to be reparameterized to be a unified linear combination of growth factors with multiple approaches available to realize it (Harring et al., 2006; Grimm et al., 2016). In this article, we express the repeated measurements of the outcome as we did in Equation (3) and accordingly write the reparameterized growth factors and the corresponding factor loadings as

$$\eta'_i = \begin{pmatrix} \eta'_{0i} & \eta'_{1i} & \eta'_{2i} \end{pmatrix}^T = \begin{pmatrix} \eta_{0i} + \gamma\eta_{1i} & \frac{\eta_{1i} + \eta_{2i}}{2} & \frac{\eta_{2i} - \eta_{1i}}{2} \end{pmatrix}^T \quad (15)$$

and

$$\Lambda'_i(\gamma) = \begin{pmatrix} 1 & t_{ij} - \gamma & |t_{ij} - \gamma| \end{pmatrix} \quad (j = 1, \dots, J). \quad (16)$$

The transformation and inverse-transformation matrices are also reduced accordingly. Specifically, we only need the first three rows and the first three columns in such matrix functions as \mathbf{G} , \mathbf{G}^{-1} , $\nabla\mathbf{G}$ and $\nabla\mathbf{G}^{-1}$, since only three growth factors need to be reparameterized. It is noted that the population-level (inverse-) transformation matrix is the same as the individual-level (inverse-) transformation matrix for the reduced model.

For the i^{th} individual, the expected mean vector and the variance-covariance matrix of the repeated outcomes of this model are

$$\mu_i = \Lambda'_i(\gamma)(\alpha' + \mathbf{B}'\mu_{\mathbf{X}}) \quad (17)$$

and

$$\Sigma_i = \Lambda'_i(\gamma)\Psi_{\eta'}\Lambda'_i(\gamma)^T + \Lambda'_i(\gamma)\mathbf{B}'\Phi\mathbf{B}'^T\Lambda'_i(\gamma)^T + \theta_\epsilon\mathbf{I}, \quad (18)$$

respectively, in which the dimensions of α' and \mathbf{B}' are 3×1 and $3 \times c$ (i.e., the first three rows of such in Equations (8) and (9)), respectively. For this reduced model, Θ_2 and Θ'_2 are defined as

$$\begin{aligned} \Theta_2 &= \{\alpha, \gamma, \Psi_{\eta}, \mathbf{B}, \mu_{\mathbf{X}}, \Phi, \theta_\epsilon\} \\ &= \{\mu_{\eta_0}, \mu_{\eta_1}, \mu_{\eta_2}, \gamma, \psi_{00}, \psi_{01}, \psi_{02}, \psi_{11}, \psi_{12}, \psi_{22}, \mathbf{B}, \mu_{\mathbf{X}}, \Phi, \theta_\epsilon\} \end{aligned} \quad (19)$$

and

$$\begin{aligned} \Theta'_2 &= \{\alpha', \gamma, \Psi_{\eta'}, \mathbf{B}', \mu_{\mathbf{X}}, \Phi, \theta_\epsilon\} \\ &= \{\mu'_{\eta_0}, \mu'_{\eta_1}, \mu'_{\eta_2}, \gamma, \psi'_{00}, \psi'_{01}, \psi'_{02}, \psi'_{11}, \psi'_{12}, \psi'_{22}, \mathbf{B}', \mu_{\mathbf{X}}, \Phi, \theta_\epsilon\}, \end{aligned} \quad (20)$$

and list the parameters in the original and reparameterized setting, respectively. By replacing Θ'_1 in Equations (12) and (13) with Θ'_2 and updating μ_i and Σ_i as such defined in Equations (17) and (18), we have the likelihood function of each individual and that of the overall sample. We build the reduced model using the R package *OpenMx* with the optimizer CSOLNP and employ the FIML technique to estimate the parameters. We provide the *OpenMx* syntax for the proposed BLSGM-TICs and its reduced version as well as a demonstration in the online appendix (https://github.com/Veronica0206/Dissertation_projects). For the researchers who are interested in using *Mplus*, we also provide *Mplus* 8 syntax for both models in the online appendix.

3 Model Evaluation

The proposed models were evaluated using a Monte Carlo simulation study with two goals. The first goal was to evaluate how the approximation led by population-level instead of individual-level inverse-transformation matrix affects the estimating effects by examining the bias ($Bias_{\hat{\theta}}(\hat{\theta}, \theta) = E_{\hat{\theta}}(\hat{\theta} - \theta)$), RMSE ($RMSE_{\hat{\theta}}(\hat{\theta}, \theta) = \sqrt{E_{\hat{\theta}}(\hat{\theta} - \theta)^2}$), as well as the empirical coverage for a nominal 95% confidence interval of each parameter of interest. The second goal was to investigate conditions under which the full BLSGM-TICs outperforms the reduced BLSGM-TICs.

3.1 Design of Simulation Study

It is known that the mean vector and variance-covariance matrix of the first three growth factors (i.e., the intercept and two slopes) usually change with the measurement scale and time scale in practice. As shown in Table 1, accordingly, we simply fixed the mean of intercept and first slope mean but changed that of the second slope to evaluate how the standardized difference between two slopes affect model performance. It is noted that we considered both positive and negative differences ($\eta_1 < \eta_2$ and $\eta_1 > \eta_2$, respectively) to assess model performance in the two cases as shown in Figure 1. For each case, we considered 3 levels of standardized difference between two slopes to evaluate the proposed models. We also fixed the variance-covariance matrix of the first three growth factors and kept the index of dispersion (σ^2/μ) of each at a tenth scale, guided by previous simulation studies for growth models (Bauer and Curran, 2003; Kohli, 2011; Kohli et al., 2015b). Further, the growth factors were set to be positively correlated to a moderate degree ($\rho = 0.3$).

=====
 Insert Table 1 about here
 =====

In addition, we chose 6 and 10 as two different levels of the number of repeated measures: 6-waves was selected as the minimum number of the repeated measures to make the model fully identified³ while 10-waves was to allow for examination of the effect of increasing the number of measurement occasions. We then let the time-window of individual measurement occasions ranging between -0.25 and $+0.25$ around each wave, which was viewed as a ‘medium’ deviation as an existing simulation study (Coulombe et al., 2015). Moreover, for the study duration with 10 records, we assessed the effect of the knot location by investigating conditions with the midway knot, left-shifted knot, and right-shifted knot. Additionally, we investigated 3 levels of magnitude of true between-person difference in the knot to compare the full to the reduced model and evaluate the effect of the approximation introduced by the population level inverse-transformation matrix. We also considered two levels of effects of exogenous variables on endogenous growth factors⁴, and two levels of measurement precision as shown in Table 1.

3.2 Data Generation and Simulation Step

For each condition which is listed in Table 1, the general steps of the simulation study for the BLSGMs-TICs with an unknown knot in the ITPs framework were carried out as follows:

1. Generated data for growth factors and TICs simultaneously using the R package *MASS* (Venables and Ripley, 2002) (details are provided in Appendix A.5).
2. Generated the time structure with J scaled and equally-spaced waves t_j and obtained ITPs: $t_{ij} \sim U(t_j - \Delta, t_j + \Delta)$ by allowing disturbances around each wave.
3. Calculated factor loadings, which are functions of ITPs and the knot, for each individual.
4. Calculated values of the repeated outcomes based on growth factors, factor loadings, and residual variances.
5. Implemented the BLSGMs-TICs with an unknown knot on simulated data, estimated the parameters, constructed corresponding 95% Wald CIs.
6. Replicated the above steps until after obtaining 1,000 convergent solutions.

4 Result

4.1 Model Convergence and Proper Solution

Before evaluating model performance, we first examined the convergence rate and component fit measures of each condition. The convergence⁵ rate of each condition was investigated. Based on our simulation studies, the proposed BLSGM-TICs and its reduced version converged satisfactorily (the convergence rate achieved 100% for $\sim 90\%$ conditions while at least 95% for other scenarios).

=====
 Insert Table 2 about here
 =====

We also conducted diagnostics to investigate improper solutions, such as estimates of growth factor variances that are less than 0, and/or estimates of correlations between growth factors are beyond $[-1, 1]$. Table 2 demonstrates the number of improper solutions yielded by the proposed model under conditions with 10 repeated measures, the knot midway through the total time of observation, and 13% explained variance of the latent growth factors, which include negative knot variances and its out-of-range (i.e., out of $[-1, 1]$) correlations with any other growth factors. When the population value of the knot variance was 0 or relatively small (i.e., $sd(\gamma) = 0.3$), the number of improper solutions was relatively large.

For the scenarios including knots with variability, we observed that the proper solution rate has positive associations with the magnitude of standardized difference, the measurement precision, the sample size, and the knot standard

³It has been proved that the bilinear latent growth model with a specified knot can be identified with at least five waves of data (Bollen and Curran, 2005).

⁴We let the TICs explain moderate (13%) and substantial (26%) variances of such factors (Cohen, 1988).

⁵In our project, convergence is defined as to achieve *OpenMx* status code 0, which suggests a successful optimization, until up to 10 attempts with different sets of starting values (Neale et al., 2016).

deviation. The sign of d_z seemed not to affect the number of improper solution meaningfully. However, the shifted knot locations or the proportion of explained variance of latent growth factors did not affect the rate of improper solution meaningfully but that reduced follow-up time inflated this number. When such improper solutions emerged, we replaced the BLSGM-TICs with its reduced version for the model evaluation.

4.2 Estimating Effects

Tables 3 and 4 present the median (range) of the bias and RMSE⁶, respectively, for each parameter of interest across all conditions for the proposed BLSGM-TICs and its reduced version. We first calculated the bias/RMSE of each parameter across 1,000 replications under each condition and then summarized the biases/RMSEs of each parameter over all the conditions as the bias/RMSE median (range). As shown in Tables 3 and 4, both models generated unbiased point estimates with small RMSEs for the mean vector though the biases and RMSEs of path coefficients were relatively large. It is also noted that the ranges of biases/RMSEs of the parameters from the full model were narrower than those from the reduced model, especially for the path coefficients and corresponding unexplained variances of latent growth parameters, indicating that the full model yielded estimates which were closer to the population values generally. On further investigation, the reduced BLSGM-TICs seemed to estimate the mean vector, the path coefficients, and the unexplained variances as precisely as the proposed full BLSGM-TICs.

=====
 Insert Table 3 about here
 =====

=====
 Insert Table 4 about here
 =====

For each parameter of interest, Figures B.1, B.2, B.3, B.4 and B.5 in Appendix B plot the biases produced by both models under conditions with 10 waves and midway knots. From those plots, we noticed the following interesting patterns. Firstly, the biases of estimates generated by both models inflated with the increase of knot variance. Secondly, though both models generated biased estimates under the conditions with considering knot variance, the biases produced by the full model were much smaller than those generated by the reduced model, especially for the path coefficients and unexplained growth factor variances. Thirdly, we noticed that the biases of the path coefficients and those of corresponding residuals exhibited sorts of ‘complementary’ relationship—the biases which had belonged to the growth factor variances ‘transferred’ to the corresponding path coefficients. Additionally, we noticed that the unexplained variances of latent growth factors of the full model were biased downwards in general, which aligns with the results from the mixed-effects model via the maximum likelihood estimation technique (Hedeker and Gibbons, 2006). Further, a larger standardized difference between two slopes, a smaller number of follow-up time, and a left- or right-shifted knot only affect biases slightly.

The RMSE of each parameter of interest demonstrated a similar association with the knot standard deviation as well as the standardized difference between two slopes. Specifically, it positively related to the magnitude of d_z and the knot standard deviation. In addition, it showed a negative association with sample size but a positive association with measurement precision. The RMSEs of the path coefficients and corresponding residual showed a ‘complementary’ relationship for the reduced BLSGM-TICs like the biases though the full BLSGM-TICs did not show such patterns.

Both BLSGMs-TICs exhibited proper coverage probabilities (CPs) (i.e., the CPs were about 0.95) under the condition without considering the knot variance while the full model covered better under the other conditions. In the non-zero knot standard deviation scenarios, we noticed that the nominal confidence intervals were also affected by factors such as the sample size and the standardized difference between two slopes. More detailed patterns concerning CPs of parameters of interest were provided in Figures B.6, B.7, B.8 and B.9 in Appendix B.

5 Application

This section demonstrates the use of proposed BLSGM-TICs to approximate nonlinear trajectories and estimate a knot that varies across individuals. This application has two goals. The first goal is to compare the fitness of bilinear spline functional form to that of three common parametric change patterns: linear, quadratic and Jenss-Bayley growth

⁶As the simulation design, the model performance under the conditions with 0 population value of the knot variance is of interest. It is noted that, under such conditions, the relative bias (RMSE) of the knot variance would go infinity. We then presented absolute biases (RMSEs) of all parameters for consistency.

curve. The second goal is to show the scenarios under which we should employ the full BLSGM-TICs instead of its reduced version in practice. We randomly selected 400 students from the Early Childhood Longitudinal Study Kindergarten Cohort: 2010-11 (ECLS-K: 2011) with complete records of repeated math IRT scaled scores, demographic information (sex, race, and age at each wave), school information (baseline school location and baseline school type), and social-economic status (baseline family income and the highest education level between parents)⁷.

ECLS-K: 2011 is a nationally representative longitudinal sample of US children enrolled in about 900 kindergarten programs starting from 2010 – 2011 school year. Children’s mathematical ability was assessed in nine waves: fall and spring of kindergarten (2010 – 2011), first (2011 – 2012) and second (2012 – 2013) grade, respectively, as well as spring of 3rd (2014), 4th (2015) and 5th (2016), respectively. Only about 30% students were sampled in the fall of 2011 and 2012 (Lê et al., 2011). In the analysis, we used children’s age (in month) instead of their grade to obtain individual measurement occasions. In the subsample, 51% of children were male, and 49% of children were female. Additionally, 45% of students were White, 5% were Black, 38% were Hispanic, 8% were Asian, and 4% were others. For this analysis, we dichotomized the variable race to be White (45%) and others (55%). At the start of the study, 11% and 89% students were in private and public school, respectively; 31%, 50%, 4% and 16% students were from a school located in city, suburb, town and rural areas, respectively. We treated the variable the highest parents’ education (ranged between 0 and 8) and family income (ranged between 1 and 18) as continuous variables, and corresponding mean (SD) was 5.18 (2.10) and 11.56 (5.42), respectively.

We first fit the full and reduced bilinear spline growth curve models as well as three parametric growth curve functions, linear, quadratic and Jenss-Bayley. The graphical representations of the model implied curves on the smooth line of the observed math IRT scores are shown in Figure 2. From the figure, the nonlinear functional forms fit better than the linear function generally; and the models with bilinear spline change patterns fit better than the parametric nonlinear models to the first two or three measurement occasions. As shown in Figure 2, both the quadratic growth curve and the Jenss-Bayley tended to underestimate the math achievement of children in the early stage.

=====
 Insert Figure 2 about here
 =====

Table 5 provides the obtained estimated likelihood, information criteria (including AIC and BIC), residuals of each latent growth curve model. From the table, the BLSGM with a random knot has the largest estimated likelihood, smallest AIC and smallest residual though its BIC is slightly larger than that of the quadratic function, which is not surprising since BIC places a larger penalty on the number of parameters. Moreover, from Table 5, the full BLSGM consistently performs better than its reduced version for this empirical example, indicating that we need to consider the variability of the knot, although the model implied trajectory of both captures the overall observed data well as shown in Figure 2. We then fit the full BLSGM-TICs to investigate the impact on the knot variance (and other growth factor variances) of covariates such as sex, race, parents’ highest education (baseline), family income (baseline), school type (baseline), and school location (baseline). Its model fit information is also provided in Table 5.

=====
 Insert Table 5 about here
 =====

=====
 Insert Table 6 about here
 =====

Table 6 presents the estimates of parameters of interest. It is noticed that post-knot development in mathematics skills slowed down substantially (on average 1.731 and 0.689 per month in the pre- and post-knot stage, respectively). The knot was estimated at 102 month on average. We noted that the initial mathematics performance (60-month old in our case) was positively associated with family income, private school, and parents’ highest education. Moreover, the family income also can explain the individual difference in the development rate of math IRT scores in the first stage. Further, boys improved more rapidly than girls in terms of math ability in the first stage. Additionally, children coming from schools from rural areas arrived at the inflection point later.

⁷The total sample size of ECLS-K: 2011 is $n = 18174$. The number of entries after removing records with missing values (i.e., rows with any of NaN/-9/-8/-7/-1) is $n = 2290$.

6 Discussion

In this article, we proposed a pair of BLSGMs-TICs for estimating an inflection point in the framework of individual measurement occasions. In both models, we viewed characteristics of the knot—its location and spread—as parameters to provide a more flexible approach to examine piecewise linear-linear change patterns. The proposed full BLSGM-TICs allows us to estimate the location of the knot rather than pre-specify it and then examine the predictors of the between-individual differences in the knot. Its reduced version provides a parsimonious option for the scenario in which such between-person differences in the knot are not significant. More importantly, we performed in-depth analyses concerning the non-convergent rate, improper solutions, as well as the bias, RMSE, and coverage probability of each parameter through simulation studies. The proposed methods were also illustrated using an empirical data set obtained from a longitudinal study of mathematics ability and compared with three common functional forms of trajectory. The results demonstrate valuable capabilities of estimating the knot with considering its variability and investigating exogenous variables to explain the between-person difference in the knot in the framework of individual measurement occasions as well as interpreting the estimates from the models.

Across all conditions that we considered in the simulation design, both models converged satisfactorily—the convergence rate of the full BLSGM-TICs achieved 100% for $\sim 90\%$ conditions while at least 95% for others while the rate of the reduced BLSGM-TICs was always 100%. Accordingly, in real practice, we recommend employing the reduced version if the full model fails to converge, though it is rare. Additionally, as shown in the application section, the full BLSGM-TICs was capable of achieving convergence status without computational burdens, even if we tested 6 time-invariant covariates simultaneously.

Of the 1,000 replications with convergent solutions across all conditions, we first examined the rate of improper solutions. Under the conditions with zero knot standard deviation, the full BLSGM-TICs suffered the improper solution issue: either negative knot variances or out-of-range correlations of the knot with other growth factors (i.e., the intercept and two slopes). This is not surprising since the full model was misspecified under the ‘true’ fixed knot conditions. Accordingly, we recommend employing the reduced BLSGM-TICs, which only estimates the knot itself, if improper solutions emerge when analyzing real-world data.

We also evaluated performance in terms of the point estimate and the coverage probability of each parameter of interest. Generally, the reduced BLSGM-TICs with an unknown knot performed well and generated desirable point estimates and coverage probabilities under the conditions without considering the knot variance. In contrast, the full BLSGM-TICs for estimating a knot and its variance, which generally performed better than the reduced model concerning point estimates and coverage probabilities in the other scenarios, were capable of yielding unbiased and precise point estimates and appropriate coverage probability. Additionally, increased follow-up time enhanced the performance of both models in general; the left-shifted knot made the estimates of the parameters of the first slope worse but those of the second slope better while the right-shifted knot worked oppositely.

Moreover, we noticed that the unexplained growth factor variances and path coefficients of the full model were underestimated generally, especially when the knot variance was relatively large, which could either be the results of employing the maximum likelihood estimation approach or be the consequence of the approximation introduced by the Taylor series expansion and the inverse-transformation matrices of the population-level. The biased upward estimates of unexplained growth factor variances of the reduced model under the condition with a random knot could be simply due to the model misspecification.

We next demonstrated the use of the proposed methods on a subset with $n = 400$ from ECLS-K: 2011 with a hope to show the procedure and provide a set of recommendations for possible issues that researchers may face in a real-world data analysis. First of all, we recommend selecting a proper functional form to depict trajectories before identifying the possible time-invariant covariates to explain the between-individual difference in the within-individual change, though this selection is not straightforward. Many factors, such as the research question, the fit between the model implied and the observed trajectory, and the information criteria, drive this selection process. It is worth to consider either the full or the reduced version of BLSGM to estimate the knot if it is the research interest. If the interest lies in to fit nonlinear trajectories, it may be appropriate to fit the change patterns with several functional forms and then select the ‘best’ one. It is noted that the fit information, sometimes, fails to lead unequivocal selection as in our empirical example. Although either the full BLSGM or the quadratic functional forms can be viewed as an ‘acceptable’ model, the full BLSGM is better if it is important to capture children’s mathematics achievement in the early stage of the study. The selection between the full and the reduced version of BLSGM can only rely on the information criteria such as BIC as they usually fit the trajectories equally, as shown in Figure 2.

One issue with using linear spline models is that the knot locations at which the change in the process has occurred must be determined, either be pre-specified, or be detected automatically, or be estimated in a much more flexible framework. Pre-specifying the knot location, which is usually driven by theory, is a popular strategy used by researchers. For

example, when the measurements are obtained from patients recovering from a certain treatment, the knot denotes the transition from the short-term to the long-term recovery period. However, in exploratory studies lacking such domain theories, it is not a straightforward task to specify the knot location *a priori*. Automated detecting a knot location is a valuable procedure for fitting linear spline models with an assumption that a knot occurs at measurement occasions. Although this assumption in empirical studies is valid if the time interval between any two adjacent measurements is reasonably short, the computational burden would be extremely intensive in the framework of individual measurement occasions.

In this article, we focused on the growth model with a bilinear spline functional form because it is the most straightforward and intuitive but useful. It can be generalized to a linear spline with multiple knots or a nonlinear spline (such as a linear-polynomial piecewise), which may also demonstrate useful in practice. Besides, it is accessible to extend the current work to address longitudinal studies with dropout under the assumption of missing at random thanks to the FIML technique. Moreover, we introduced approximations when replacing the individual-level inverse-transformation matrices with the population-level inverse-transformation matrices. The individual-level inverse-transformation matrices are also realizable with a more complicated process if more unbiased and precise estimates are desirable. Additionally, we focused on time-invariant covariates in the current work, which is helpful to identify baseline characteristics to explain the variability of growth factors. It can also be extended to investigate time-varying covariates to explain the individual-difference in the trajectories.

Appendix A Formula Derivation

A.1 Taylor Series Expansion

For the i^{th} individual, suppose we have a function $f(\gamma_i)$ and its first derivative with respect to γ_i ⁸, shown in equations

$$f(\gamma_i) = \eta'_{0i} + \eta'_{1i}(t_{ij} - \gamma_i) + \eta'_{2i}\sqrt{(t_{ij} - \gamma_i)^2}$$

and

$$f'(\gamma_i) = \eta_{1i} - \eta'_{1i} - \frac{\eta'_{2i}(t_{ij} - \gamma_i)}{\sqrt{(t_{ij} - \gamma_i)^2}} = -\eta'_{2i} - \frac{\eta'_{2i}(t_{ij} - \gamma_i)}{\sqrt{(t_{ij} - \gamma_i)^2}},$$

respectively. Then the Taylor series expansion of $f(\gamma_i)$ can be expressed as

$$\begin{aligned} f(\gamma_i) &= f(\mu_\gamma) + \frac{f'(\mu_\gamma)}{1!}(\gamma_i - \mu_\gamma) + \dots \\ &= \eta'_{0i} + \eta'_{1i}(t_{ij} - \mu_\gamma) + \eta'_{2i}\sqrt{(t_{ij} - \mu_\gamma)^2} + (\gamma_i - \mu_\gamma) \left[-\eta'_{2i} - \frac{\eta'_{2i}(t_{ij} - \mu_\gamma)}{|t_{ij} - \mu_\gamma|} \right] + \dots \\ &\approx \eta'_{0i} + \eta'_{1i}(t_{ij} - \mu_\gamma) + \eta'_{2i}|t_{ij} - \mu_\gamma| + (\gamma_i - \mu_\gamma) \left[-\mu_{\eta'_2} - \frac{\mu_{\eta'_2}(t_{ij} - \mu_\gamma)}{|t_{ij} - \mu_\gamma|} \right], \end{aligned}$$

from which we then have the reparameterized growth factors and the corresponding factor loadings for the i^{th} individual.

A.2 Derivation of transformation matrices and the inverse-transformation matrices between mean vectors and variance-covariance matrices at the population-level

Through straightforward algebra, we can approximate the mean vector of the reparameterized growth factors from the mean vector of their original setting via the following equation

$$\begin{aligned} \boldsymbol{\mu}_{\boldsymbol{\eta}'} &= E(\mathbf{G}_i \times \begin{pmatrix} \eta_{0i} \\ \eta_{1i} \\ \eta_{2i} \\ \gamma_i - \mu_\gamma \end{pmatrix}) = E \left[\begin{pmatrix} 1 & \gamma_i & 0 & 0 \\ 0 & 0.5 & 0.5 & 0 \\ 0 & -0.5 & 0.5 & 0 \\ 0 & 0 & 0 & 1 \end{pmatrix} \times \begin{pmatrix} \eta_{0i} \\ \eta_{1i} \\ \eta_{2i} \\ \gamma_i - \mu_\gamma \end{pmatrix} \right] \\ &\approx \begin{pmatrix} 1 & \mu_\gamma & 0 & 0 \\ 0 & 0.5 & 0.5 & 0 \\ 0 & -0.5 & 0.5 & 0 \\ 0 & 0 & 0 & 1 \end{pmatrix} \times \begin{pmatrix} \mu_{\eta_0} \\ \mu_{\eta_1} \\ \mu_{\eta_2} \\ 0 \end{pmatrix} \end{aligned}$$

under the condition of $\frac{1}{n} \sum_{i=1}^n Cov(\eta_{1i}, \gamma_i) \rightarrow 0$.

Similarly, the mean vector of the original parameters can be approximated from the reparameterized setting through the equation

$$\begin{aligned} \boldsymbol{\mu}_\boldsymbol{\eta} &= E(\mathbf{G}_i^{-1} \times \begin{pmatrix} \eta'_{0i} \\ \eta'_{1i} \\ \eta'_{2i} \\ \delta_i + \mu_\gamma \end{pmatrix}) = E \left[\begin{pmatrix} 1 & -\gamma_i & \gamma_i & 0 \\ 0 & 1 & -1 & 0 \\ 0 & 1 & 1 & 0 \\ 0 & 0 & 0 & 1 \end{pmatrix} \times \begin{pmatrix} \eta'_{0i} \\ \eta'_{1i} \\ \eta'_{2i} \\ \delta_i + \mu_\gamma \end{pmatrix} \right] \\ &\approx \begin{pmatrix} 1 & -\mu_\gamma & \mu_\gamma & 0 \\ 0 & 1 & -1 & 0 \\ 0 & 1 & 1 & 0 \\ 0 & 0 & 0 & 1 \end{pmatrix} \times \begin{pmatrix} \mu_{\eta'_{0i}} \\ \mu_{\eta'_{1i}} \\ \mu_{\eta'_{2i}} \\ \mu_\gamma \end{pmatrix} \end{aligned}$$

under the condition of $\frac{1}{n} \sum_{i=1}^n Cov(\eta_{2i}, \gamma_i) \rightarrow 0$.

⁸It is noted that we have 4 degree-of-freedom when expressing the repeated outcomes of a linear combination of 4 growth factors (Harrington et al., 2006). To simplify subsequent calculation, we viewed η_{0i} , η_{1i} , η_{2i} and γ_i (i.e., the growth factors in the original setting) as independent variables. It is also noted that γ_i is intact during the process of reparameterization (Preacher and Hancock, 2012).

Through variance decomposition, we can approximate the variance-covariance matrix of the reparameterized growth factors from the variance-covariance matrix of their original setting via the following equation

$$\begin{aligned}
\Psi_{\eta'} &= \text{Var}(\mathbf{G}_i \times \boldsymbol{\eta}_i) = E(\text{Var}(\mathbf{G}_i \times \boldsymbol{\eta}_i | \gamma_i)) + \text{Var}(E(\mathbf{G}_i \times \boldsymbol{\eta}_i | \gamma_i)) \\
&\approx E(\text{Var}(\mathbf{G}_i \times \boldsymbol{\eta}_i | \gamma_i)) = E(\nabla \mathbf{G}_i \text{Var}(\boldsymbol{\eta}_i) \nabla \mathbf{G}_i^T) \\
&\approx \begin{pmatrix} 1 & \mu_\gamma & 0 & \mu_{\eta_1} \\ 0 & 0.5 & 0.5 & 0 \\ 0 & -0.5 & 0.5 & 0 \\ 0 & 0 & 0 & 1 \end{pmatrix} \Psi_{\eta} \begin{pmatrix} 1 & \mu_\gamma & 0 & \mu_{\eta_1} \\ 0 & 0.5 & 0.5 & 0 \\ 0 & -0.5 & 0.5 & 0 \\ 0 & 0 & 0 & 1 \end{pmatrix}^T \\
&= \nabla \mathbf{G} \Psi_{\eta} \nabla \mathbf{G}^T
\end{aligned} \tag{A.1}$$

under the condition of $\text{Var}(\gamma_i) \rightarrow 0$ and $\text{Var}(\eta_{1i}) \rightarrow 0$.

Similarly, the variance-covariance matrix of the original parameters can be approximated from the reparameterized setting through the equation

$$\begin{aligned}
\Psi_{\eta} &= \text{Var}(\mathbf{G}_i^{-1} \times \boldsymbol{\eta}'_i) = E(\text{Var}(\mathbf{G}_i^{-1} \times \boldsymbol{\eta}'_i | \gamma_i)) + \text{Var}(E(\mathbf{G}_i^{-1} \times \boldsymbol{\eta}'_i | \gamma_i)) \\
&\approx E(\text{Var}(\mathbf{G}_i^{-1} \times \boldsymbol{\eta}'_i | \gamma_i)) = E(\nabla \mathbf{G}_i^{-1} \text{Var}(\boldsymbol{\eta}'_i) \nabla \mathbf{G}_i^{-1T}) \\
&\approx \begin{pmatrix} 1 & -\mu_\gamma & \mu_\gamma & 0 \\ 0 & 1 & -1 & 0 \\ 0 & 1 & 1 & 0 \\ 0 & 0 & 0 & 1 \end{pmatrix} \Psi_{\eta'} \begin{pmatrix} 1 & -\mu_\gamma & \mu_\gamma & 0 \\ 0 & 1 & -1 & 0 \\ 0 & 1 & 1 & 0 \\ 0 & 0 & 0 & 1 \end{pmatrix}^T \\
&= \nabla \mathbf{G}^{-1} \Psi_{\eta'} \nabla \mathbf{G}^{-1T}.
\end{aligned} \tag{A.2}$$

under the condition of $\text{Var}(\gamma_i) \rightarrow 0$.

Through the above equations, we noticed that the most critical condition for the approximation to the population-level transformation is $\text{Var}(\gamma_i) \rightarrow 0$. With this condition, the covariances of the knot with other growth factors approach to 0. More importantly, the second item of the expression of variance decomposition in Equations (A.1) and (A.2) approaches to 0 given $\text{Var}(\gamma_i) \rightarrow 0$. Though Equation (A.1) requires $\text{Var}(\eta_{1i}) \rightarrow 0$, whether to satisfy this condition or not does not affect estimation process.

A.3 Expression of each cell of the re-reparameterized mean vector and variance-covariance matrix

$$\begin{aligned}
\mu_{\eta_0} &\approx \mu_{\eta'_0} - \mu_\gamma \mu_{\eta'_1} + \mu_\gamma \mu_{\eta'_2} \\
\mu_{\eta_1} &= \mu_{\eta'_1} - \mu_{\eta'_2} \\
\mu_{\eta_2} &= \mu_{\eta'_2} + \mu_{\eta'_1} \\
\mu_\gamma &= \mu_\gamma \\
\psi_{00} &\approx (\psi'_{11} + \psi'_{22} - 2\psi'_{12})\mu_\gamma^2 + 2(\psi'_{02} - \psi'_{01})\mu_\gamma + \psi'_{00} \\
\psi_{01} &\approx (2\psi'_{12} - \psi'_{11} - \psi'_{22})\mu_\gamma + (\psi'_{01} - \psi'_{02}) \\
\psi_{02} &\approx (\psi'_{22} - \psi'_{11})\mu_\gamma + (\psi'_{01} + \psi'_{02}) \\
\psi_{0\gamma} &\approx (\psi'_{2\gamma} - \psi'_{1\gamma})\mu_\gamma + \psi'_{0\gamma} \\
\psi_{11} &= \psi'_{11} + \psi'_{22} - 2\psi'_{12} \\
\psi_{12} &= \psi'_{11} - \psi'_{22} \\
\psi_{1\gamma} &= \psi'_{1\gamma} - \psi'_{2\gamma} \\
\psi_{22} &= \psi'_{11} + \psi'_{22} + 2\psi'_{12} \\
\psi_{2\gamma} &= \psi'_{1\gamma} + \psi'_{2\gamma} \\
\psi_{\gamma\gamma} &= \psi'_{\gamma\gamma}
\end{aligned}$$

A.4 Details of the transformation matrices and the inverse-transformation matrices between intercept coefficients and path coefficients

$$\begin{aligned}
\boldsymbol{\mu}'_{\eta} &\approx \mathbf{G} \times \boldsymbol{\mu}_{\eta} \iff E(\boldsymbol{\alpha}' + \mathbf{B}' \mathbf{X}_i) \approx \mathbf{G} \times E(\boldsymbol{\alpha} + \mathbf{B} \mathbf{X}_i) \iff \boldsymbol{\alpha}' \approx \mathbf{G} \times \boldsymbol{\alpha} \\
\boldsymbol{\mu}_{\eta} &\approx \mathbf{G}^{-1} \times \boldsymbol{\mu}'_{\eta} \iff E(\boldsymbol{\alpha} + \mathbf{B} \mathbf{X}_i) \approx \mathbf{G}^{-1} \times E(\boldsymbol{\alpha}' + \mathbf{B}' \mathbf{X}_i) \iff \boldsymbol{\alpha} \approx \mathbf{G}^{-1} \times \boldsymbol{\alpha}' \\
\boldsymbol{\Psi}'_{\eta} &\approx \nabla \mathbf{G} \boldsymbol{\Psi}_{\eta} \nabla \mathbf{G}^T \\
&\iff \text{Var}(\boldsymbol{\alpha}' + \mathbf{B}' \mathbf{X}_i + \boldsymbol{\zeta}'_i) \approx \nabla \mathbf{G} \text{Var}(\boldsymbol{\alpha} + \mathbf{B} \mathbf{X}_i + \boldsymbol{\zeta}_i) \nabla \mathbf{G}^T \\
&\iff \text{Var}(\mathbf{B}' \mathbf{X}_i + \boldsymbol{\zeta}'_i) \approx \nabla \mathbf{G} \text{Var}(\mathbf{B} \mathbf{X}_i + \boldsymbol{\zeta}_i) \nabla \mathbf{G}^T \\
&\iff \mathbf{B}' \text{Var}(\mathbf{X}_i) \mathbf{B}'^T + \text{Var}(\boldsymbol{\zeta}'_i) \approx \nabla \mathbf{G} \mathbf{B} \text{Var}(\mathbf{X}_i) \mathbf{B}^T \nabla \mathbf{G}^T + \nabla \mathbf{G} \text{Var}(\boldsymbol{\zeta}_i) \nabla \mathbf{G}^T \\
&\iff \mathbf{B}' \approx \nabla \mathbf{G} \mathbf{B} \\
\boldsymbol{\Psi}_{\eta} &\approx \nabla \mathbf{G}^{-1} \boldsymbol{\Psi}'_{\eta} \nabla \mathbf{G}^{-1T} \\
&\iff \text{Var}(\boldsymbol{\alpha} + \mathbf{B} \mathbf{X}_i + \boldsymbol{\zeta}_i) \approx \nabla \mathbf{G}^{-1} \text{Var}(\boldsymbol{\alpha}' + \mathbf{B}' \mathbf{X}_i + \boldsymbol{\zeta}'_i) \nabla \mathbf{G}^{-1T} \\
&\iff \text{Var}(\mathbf{B} \mathbf{X}_i + \boldsymbol{\zeta}_i) \approx \nabla \mathbf{G}^{-1} \text{Var}(\mathbf{B}' \mathbf{X}_i + \boldsymbol{\zeta}'_i) \nabla \mathbf{G}^{-1T} \\
&\iff \mathbf{B} \text{Var}(\mathbf{X}_i) \mathbf{B}^T + \text{Var}(\boldsymbol{\zeta}_i) \approx \nabla \mathbf{G}^{-1} \mathbf{B}' \text{Var}(\mathbf{X}_i) \mathbf{B}'^T \nabla \mathbf{G}^{-1T} + \nabla \mathbf{G}^{-1} \text{Var}(\boldsymbol{\zeta}'_i) \nabla \mathbf{G}^{-1T} \\
&\iff \mathbf{B} \approx \nabla \mathbf{G}^{-1} \mathbf{B}'
\end{aligned}$$

A.5 Generate Exogenous Variables and Growth Factors Simultaneously

To generate growth factors and exogenous variables simultaneously as a multivariate normal distribution, we need to specify the mean vector and the variance-covariance matrix of the distribution. In our setting, the mean vector can be represented in equation

$$\boldsymbol{\mu} = (\boldsymbol{\alpha} \quad 0 \quad 0),$$

where $\boldsymbol{\alpha}$ and $(0 \quad 0)$ are the mean vector of the growth factors and that of the TICs, respectively. Moreover, through straightforward linear algebra, the underlying variance-covariance matrix of the distribution is

$$\boldsymbol{\Sigma} = \begin{pmatrix} \mathbf{B}\boldsymbol{\Phi}\mathbf{B} + \boldsymbol{\Psi}_{\eta} & \mathbf{B}\boldsymbol{\Phi} \\ \mathbf{B}\boldsymbol{\Phi} & \boldsymbol{\Phi} \end{pmatrix},$$

where \mathbf{B} is the matrix of path coefficients, $\boldsymbol{\Psi}_{\eta}$ and $\boldsymbol{\Phi}$ are the variance-covariance matrices of the growth factors and the TICs, respectively. Accordingly, we can generate the growth factors and TICs simultaneously, which follows a multivariate normal distribution $N_6(\boldsymbol{\mu}, \boldsymbol{\Sigma})$.

Appendix B More Results

=====
Insert Figure B.1 about here
=====

=====
Insert Figure B.2 about here
=====

=====
Insert Figure B.3 about here
=====

=====
Insert Figure B.4 about here
=====

=====
Insert Figure B.5 about here
=====

=====
 Insert Figure B.6 about here
 =====

=====
 Insert Figure B.7 about here
 =====

=====
 Insert Figure B.8 about here
 =====

=====
 Insert Figure B.9 about here
 =====

References

- Bauer, D. J. and Curran, P. J. (2003). Distributional assumptions of growth mixture models: Implications for overextraction of latent trajectory classes. *Psychological Methods*, 8(3):338–363.
- Boker, S. M., Neale, M. C., Maes, H. H., Wilde, M. J., Spiegel, M., Brick, T. R., Estabrook, R., Bates, T. C., Mehta, P., von Oertzen, T., Gore, R. J., Hunter, M. D., Hackett, D. C., Karch, J., Brandmaier, A. M., Pritikin, J. N., Zahery, M., Kirkpatrick, R. M., Wang, Y., Driver, C., Massachusetts Institute of Technology, Johnson, S. G., Association for Computing Machinery, Kraft, D., Wilhelm, S., and Manjunath, B. G. (2018). *OpenMx 2.9.6 User Guide*.
- Bollen, K. A. and Curran, P. J. (2005). *Latent Curve Models*. John Wiley & Sons, Inc.
- Browne, M. W. and du Toit, S. H. C. (1991). Models for learning data. In Collins, L. M. and Horn, J. L., editors, *Best methods for the analysis of change: Recent advances, unanswered questions, future directions*, chapter 4, pages 47–68. American Psychological Association., Washington, DC, US.
- Cohen, J. (1988). *Statistical Power Analysis for the Behavioral Sciences (2nd Ed.)*. Lawrence Erlbaum Associates.
- Cook, N. R. and Ware, J. H. (1983). Design and analysis methods for longitudinal research. *Annual Review of Public Health*, 4(1):1–23.
- Coulombe, P., Selig, J. P., and Delaney, H. D. (2015). Ignoring individual differences in times of assessment in growth curve modeling. *International Journal of Behavioral Development*, 40(1):76–86.
- Cudeck, R. and Klebe, K. J. (2002). Multiphase mixed-effects models for repeated measures data. *Psychological Methods*, 7(1):41–63.
- Dumenci, L., Perera, R. A., Keefe, F. J., Ang, D. C., J., S., Jensen, M. P., and Riddle, D. L. (2019). Model-based pain and function outcome trajectory types for patients undergoing knee arthroplasty: a secondary analysis from a randomized clinical trial. *Osteoarthritis and cartilage*, 27(6):878–884.
- Finkel, D., Reynolds, C., Mcardle, J., Gatz, M., and L Pedersen, N. (2003). Latent growth curve analyses of accelerating decline in cognitive abilities in late adulthood. *Developmental psychology*, 39:535–550.
- Flora, D. B. (2008). Specifying piecewise latent trajectory models for longitudinal data. *Structural Equation Modeling: A Multidisciplinary Journal*, 15(3):513–533.
- Grimm, K. J., Ram, N., and Estabrook, R. (2016). *Growth Modeling*. Guilford Press.
- Harring, J. R. (2009). A nonlinear mixed effects model for latent variables. *Journal of Educational and Behavioral Statistics*, 34(3):293–318.
- Harring, J. R., Cudeck, R., and du Toit, S. H. C. (2006). Fitting partially nonlinear random coefficient models as sems. *Multivariate Behavioral Research*, 41(4):579–596.
- Hedeker, D. and Gibbons, R. D. (2006). *Longitudinal Data Analysis*. Wiley Series in Probability and Statistics. Wiley.
- Hedeker, D., Mermelstein, R. J., and Flay, B. R. (2006). Application of item response theory models for intensive longitudinal data. In Walls, T. A. and Schafer, J. L., editors, *Models for Intensive Longitudinal Data*, chapter 4, pages 84–108. Oxford University Press, ProQuest Ebook Central.
- Hunter, M. D. (2018). State space modeling in an open source, modular, structural equation modeling environment. *Structural Equation Modeling*, 25(2):307–324.

- Jones, H. E. and Bayley, N. (1941). The berkeley growth study. *Child Development*, 12:167–173.
- Kohli, N. (2011). *Estimating unknown knots in piecewise linear-linear latent growth mixture models*. PhD thesis, University of Maryland.
- Kohli, N. and Haring, J. R. (2013). Modeling growth in latent variables using a piecewise function. *Multivariate Behavioral Research*, 48(3):370–397.
- Kohli, N., Haring, J. R., and Hancock, G. R. (2013). Piecewise linear-linear latent growth mixture models with unknown knots. *Educational and Psychological Measurement*, 73(6):935–955.
- Kohli, N., Hughes, J., Wang, C., Zopluoglu, C., and Davison, M. L. (2015a). Fitting a linear-linear piecewise growth mixture model with unknown knots: A comparison of two common approaches to inference. *Psychological Methods*, 20(2):259–275.
- Kohli, N., Sullivan, A. L., Sadeh, S., and Zopluoglu, C. (2015b). Longitudinal mathematics development of students with learning disabilities and students without disabilities: A comparison of linear, quadratic, and piecewise linear mixed effects models. *Journal of School Psychology*, 53(2):105–120.
- Kwok, O., Luo, W., and West, S. G. (2010). Using modification indexes to detect turning points in longitudinal data: A monte carlo study. *Structural Equation Modeling: A Multidisciplinary Journal*, 17(2):216–240.
- Lê, T., Norman, G., Tourangeau, K., Brick, J. M., and Mulligan, G. (2011). Early childhood longitudinal study: Kindergarten class of 2010-2011 – sample design issues. *JSM Proceedings*, pages 1629–1639.
- Li, F., Duncan, T. E., Duncan, S. C., and Hops, H. (2001). Piecewise growth mixture modeling of adolescent alcohol use data. *Structural Equation Modeling: A Multidisciplinary Journal*, 8(2):175–204.
- Marcoulides, K. M. (2018). Automated latent growth curve model fitting: A segmentation and knot selection approach. *Structural Equation Modeling: A Multidisciplinary Journal*, 25(5):687–699.
- Mehta, P. D. and Neale, M. C. (2005). People are variables too: Multilevel structural equations modeling. *Psychological Methods*, 10(3):259–284.
- Mehta, P. D. and West, S. G. (2000). Putting the individual back into individual growth curves. *Psychological Methods*, 5(1):23–43.
- Neale, M. C., Hunter, M. D., Pritikin, J. N., Zahery, M., Brick, T. R., Kirkpatrick, R. M., Estabrook, R., Bates, T. C., Maes, H. H., and Boker, S. M. (2016). OpenMx 2.0: Extended structural equation and statistical modeling. *Psychometrika*, 81(2):535–549.
- Preacher, K. J. and Hancock, G. R. (2012). On interpretable reparameterizations of linear and nonlinear latent growth curve models. In Haring, J. R. and Hancock, G. R., editors, *CILVR series on latent variable methodology. Advances in longitudinal methods in the social and behavioral sciences*, chapter 2, pages 25–58. IAP Information Age Publishing, Charlotte, NC, US.
- Preacher, K. J. and Hancock, G. R. (2015). Meaningful aspects of change as novel random coefficients: A general method for reparameterizing longitudinal models. *Psychological Methods*, 20(1):84–101.
- Pritikin, J. N., Hunter, M. D., and Boker, S. M. (2015). Modular open-source software for Item Factor Analysis. *Educational and Psychological Measurement*, 75(3):458–474.
- Riddle, D. L., Perera, R. A., Jiranek, W. A., and Dumenci, L. (2015). Using surgical appropriateness criteria to examine outcomes of total knee arthroplasty in a united states sample. *Arthritis care & research.*, 67(3):349–357.
- Seber, G. A. F. and Wild, C. J. (2003). *Nonlinear Regression*. John Wiley & Sons, Inc.
- Sterba, S. K. (2014). Fitting nonlinear latent growth curve models with individually varying time points. *Structural Equation Modeling: A Multidisciplinary Journal*, 21(4):630–647.
- Tishler, A. and Zang, I. (1981). A maximum likelihood method for piecewise regression models with a continuous dependent variable. *Journal of the Royal Statistical Society. Series C. Applied Statistics*, 30.
- Venables, W. N. and Ripley, B. D. (2002). *Modern Applied Statistics with S*. Springer, New York, fourth edition.

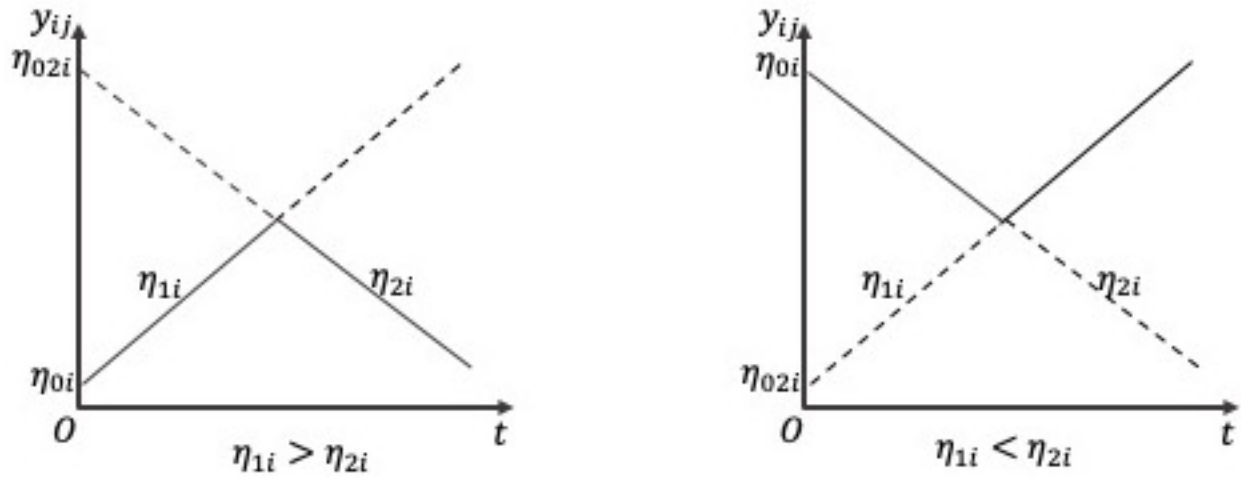


Figure 1: The Two Forms of the Bilinear Spline (Linear-Linear Piecewise)

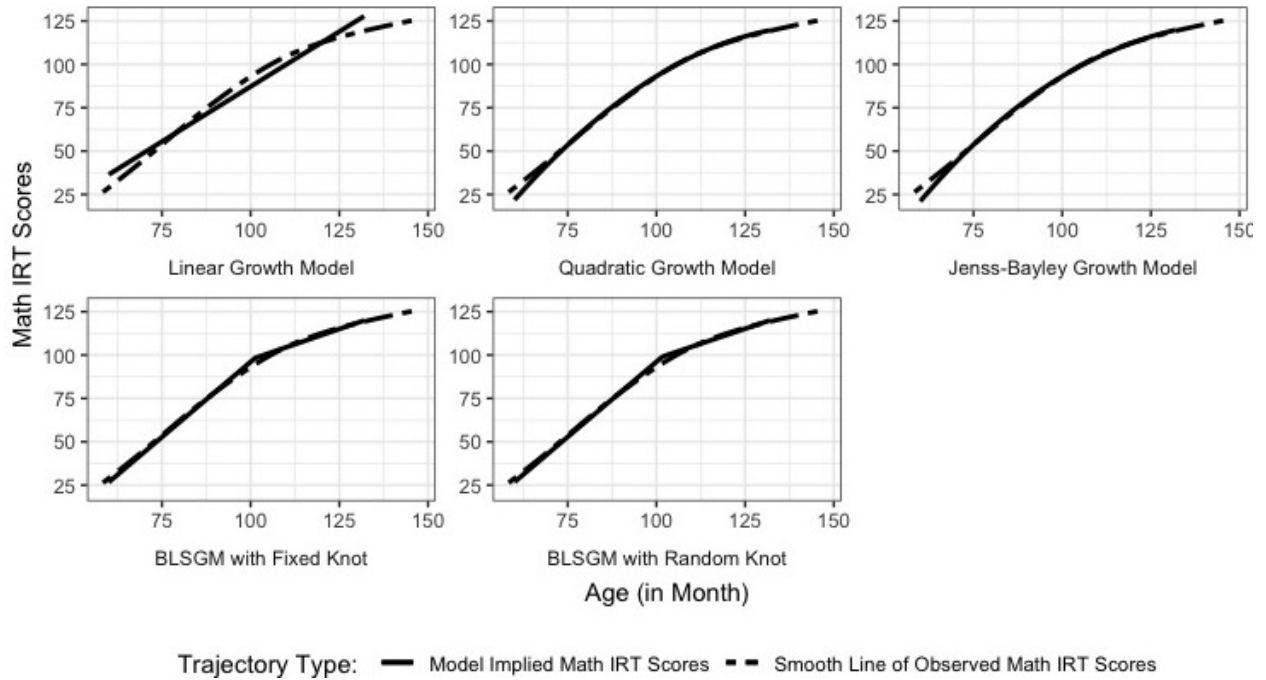


Figure 2: Model Implied Trajectory and Smooth Line of Observed Math IRT Scores

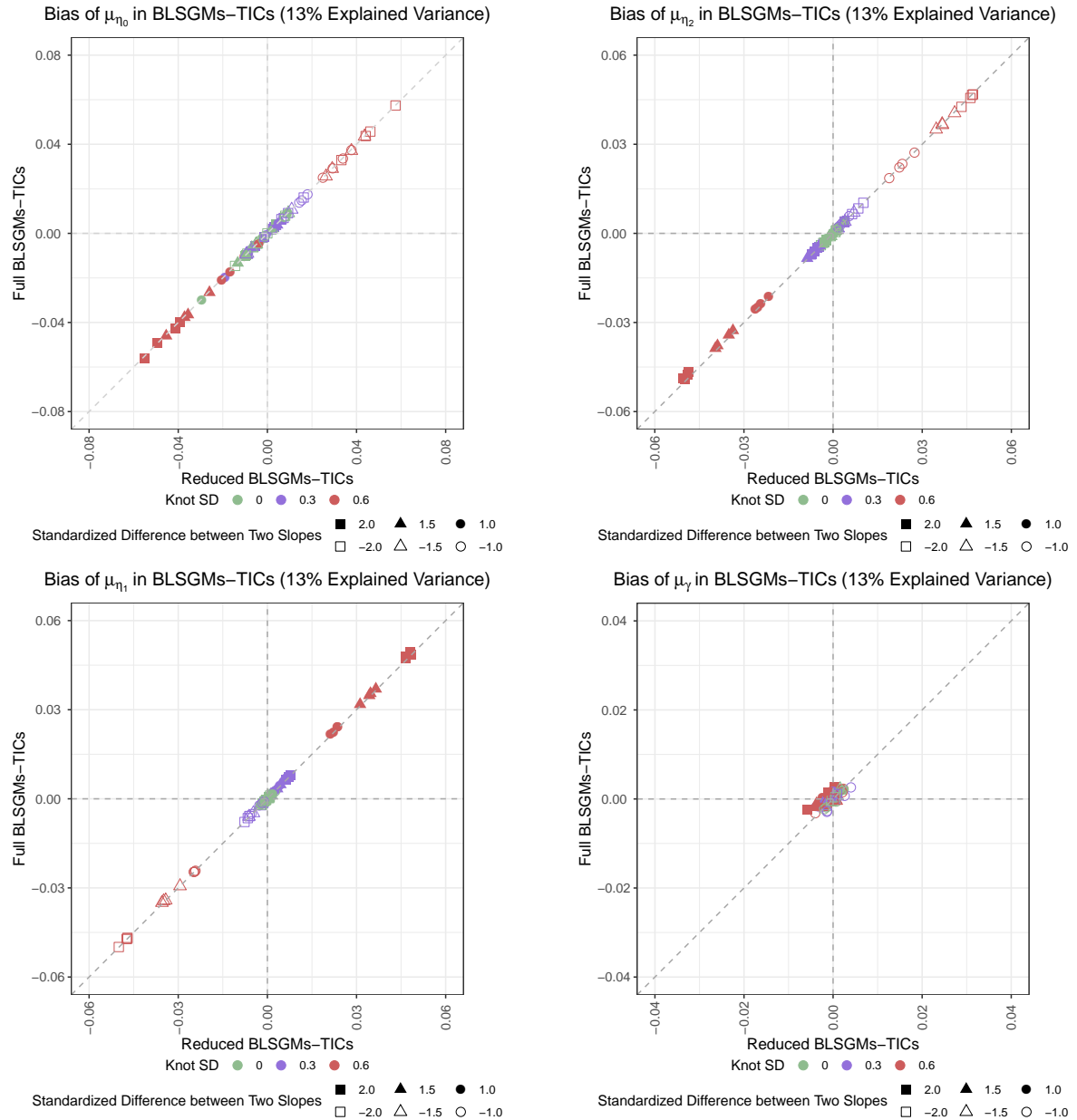


Figure B.1: Biases of Mean Vector of Growth Factors of BLSGM-TICs with in the ITPs Framework (Under Conditions with 10 Repeated Measures, Midway Knot and 13% explained variance)

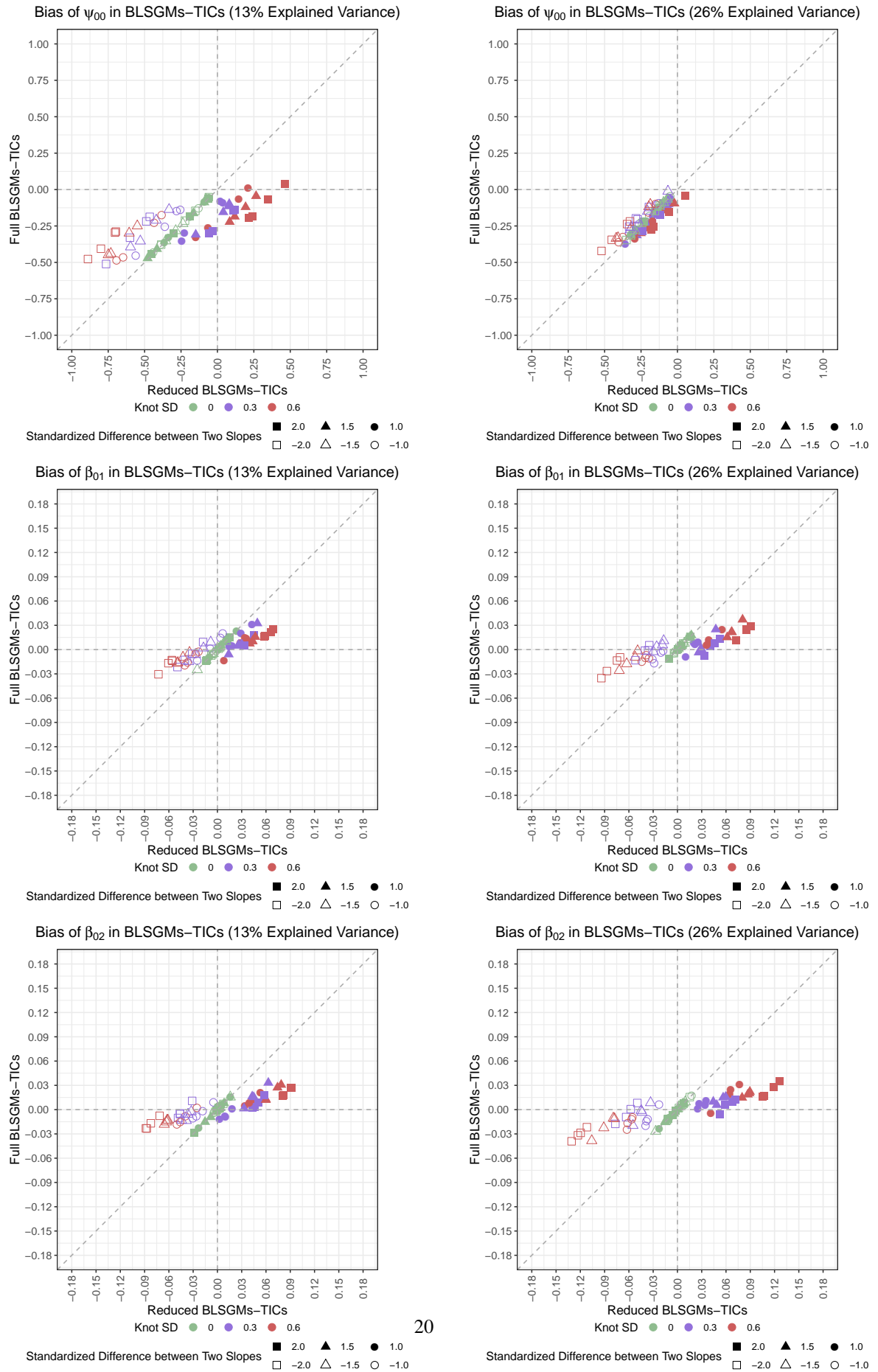


Figure B.2: Biases of Path Coefficients and Residuals of Intercept of BLSGM-TICs with in the ITPs Framework (Under Conditions with 10 Repeated Measures and Midway Knot)

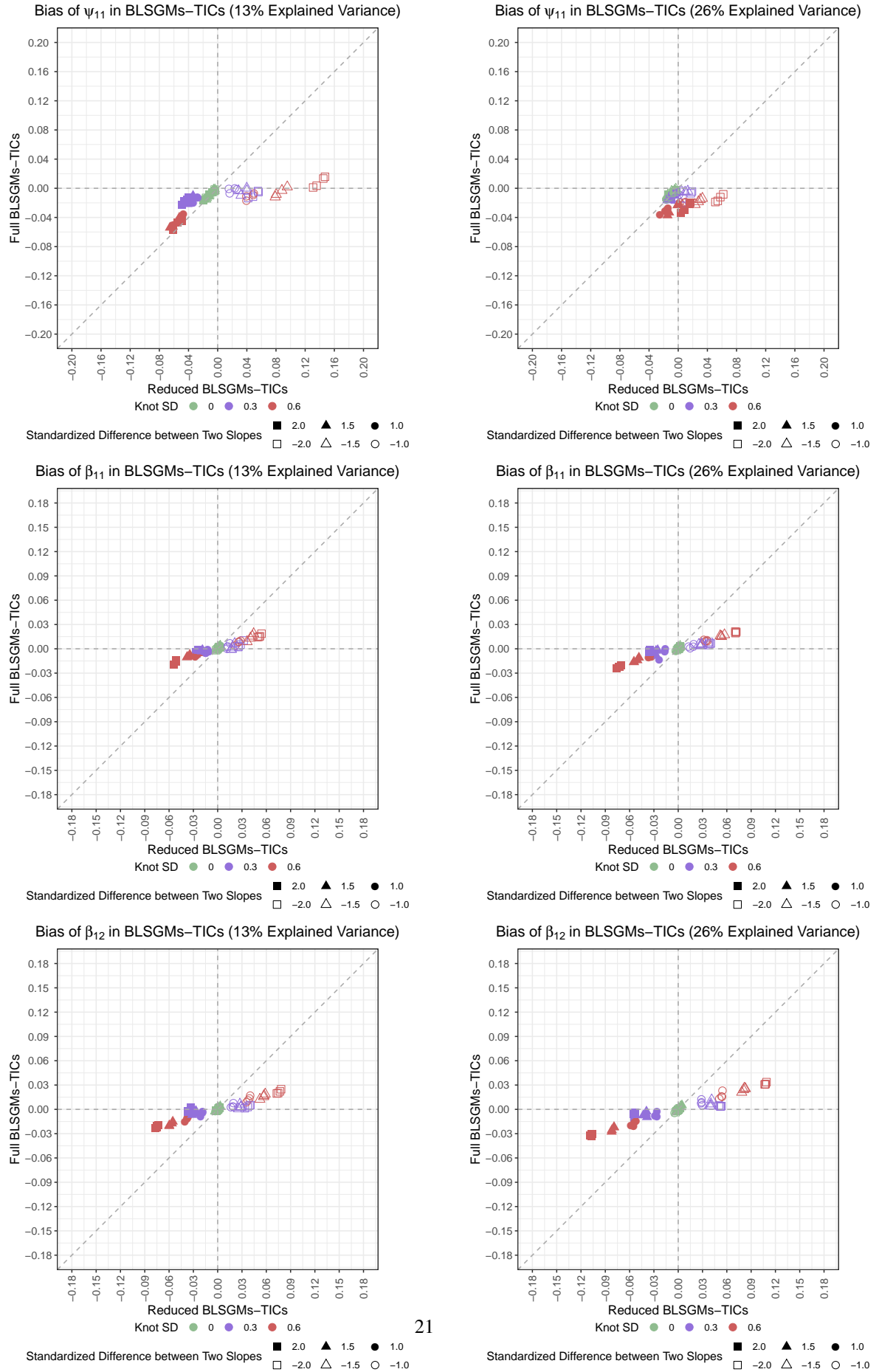


Figure B.3: Biases of Path Coefficients and Residuals of 1st Slope of BLSGM-TICs with in the ITPs Framework (Under Conditions with 10 Repeated Measures and Midway Knot)

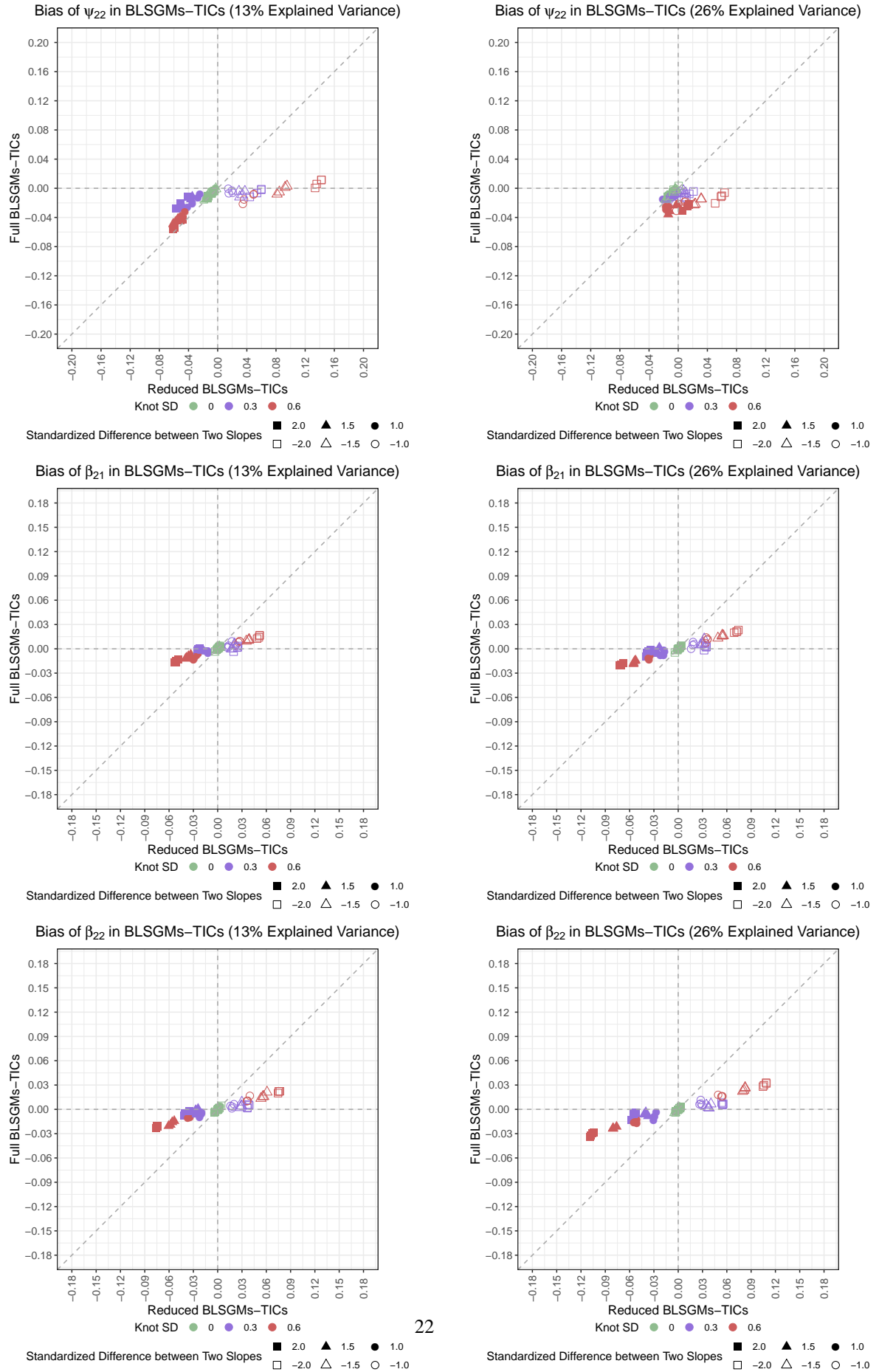


Figure B.4: Biases of Path Coefficients and Residuals of 2nd Slope of BLSGM-TICs in the ITPs Framework (Under Conditions with 10 Repeated Measures and Midway Knot)

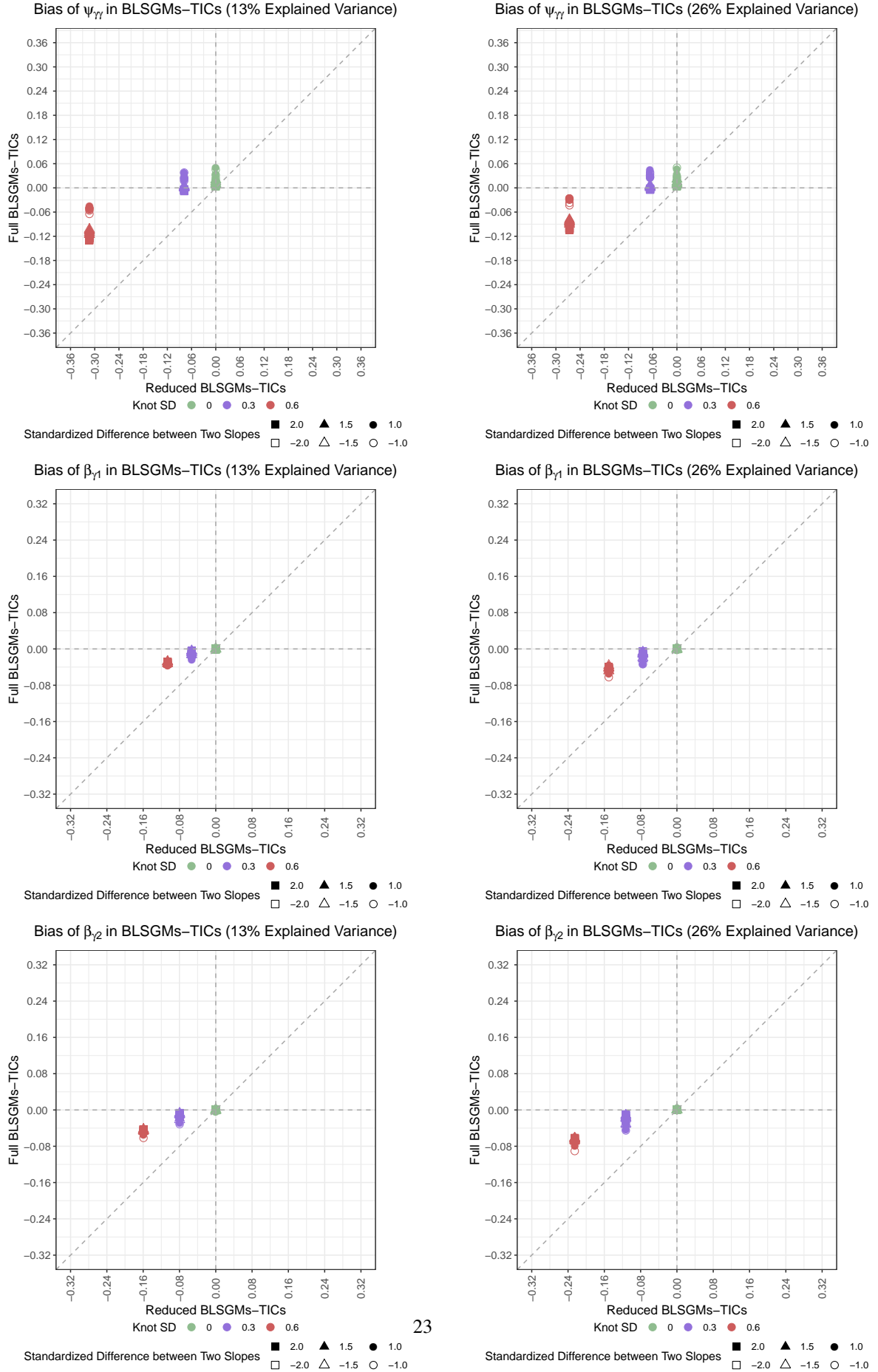


Figure B.5: Biases of Path Coefficients and Residuals of Knot for BLSGM-TICs with in the ITPs Framework (Under Conditions with 10 Repeated Measures and Midway Knot)

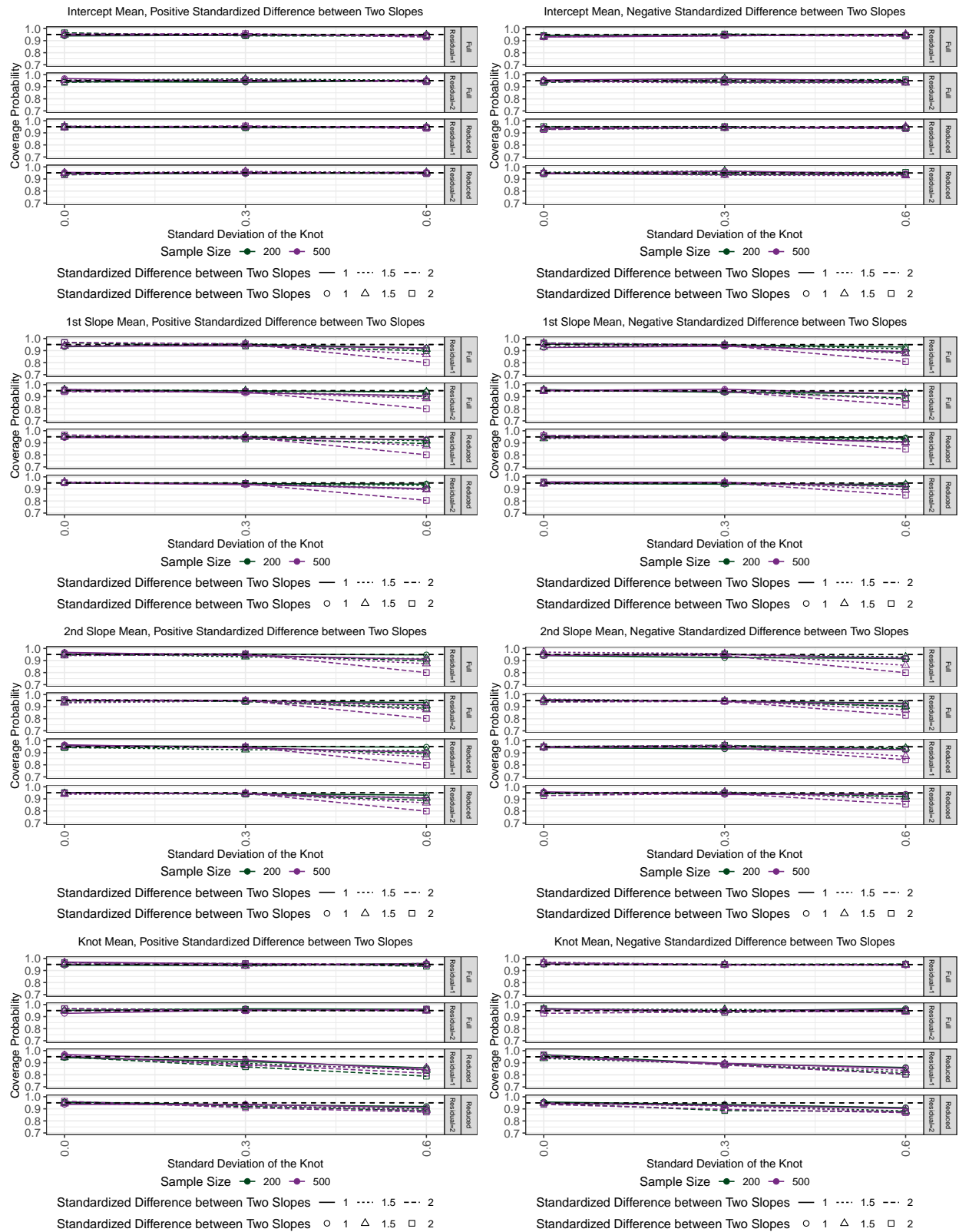


Figure B.6: Coverage Probability of Means of Latent Variables in BLSGMs-TICs in the ITPs Framework (Under Conditions with 10 Repeated Measures Midway Knot and 13% Explained Variance)

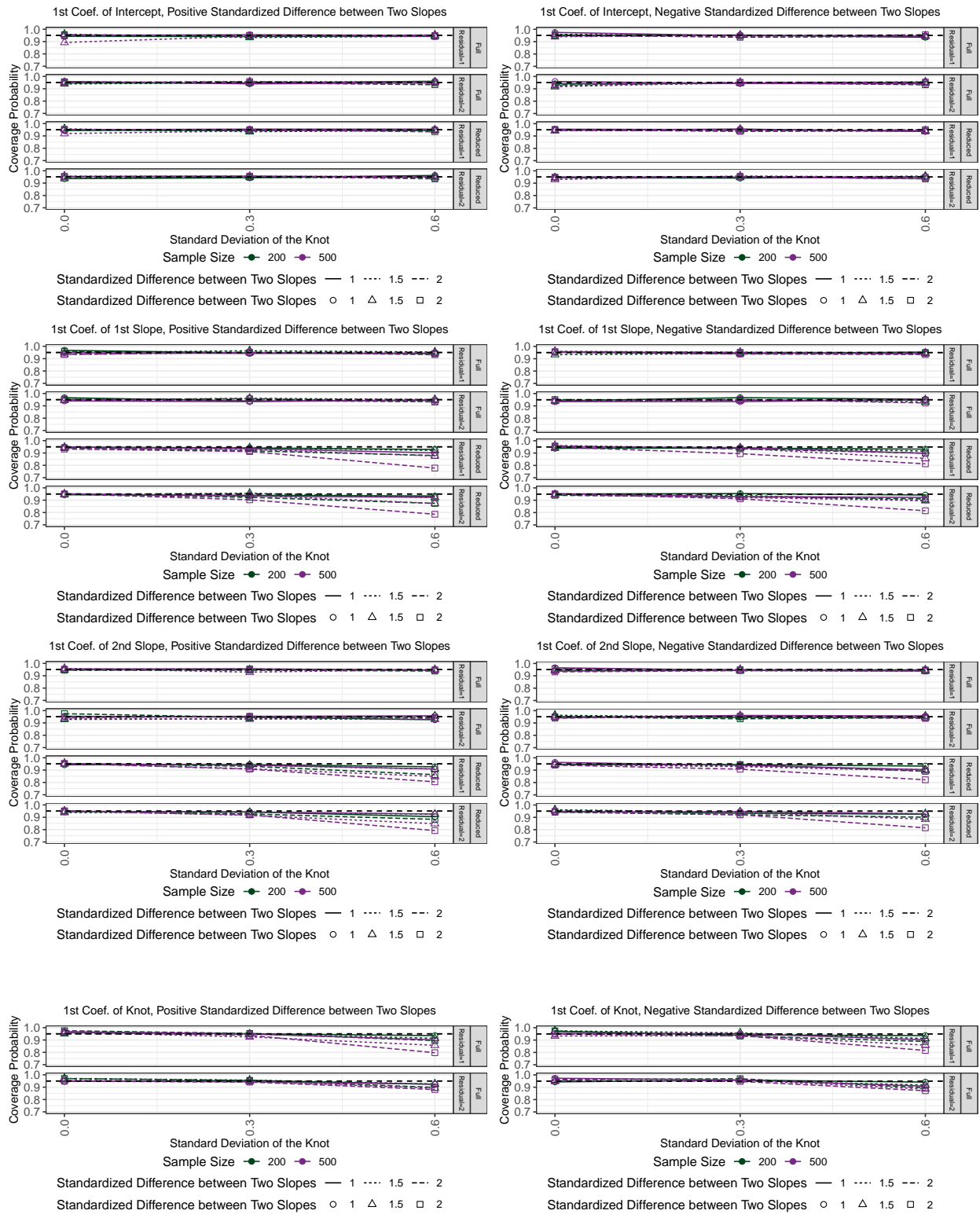


Figure B.7: Coverage Probability of Path Coefficients of x_1 in BLSGMs-TICs in the ITPs Framework (Under Conditions with 10 Repeated Measures, Midway Knot, Small Residuals and 13% Variances Explained by TICs)

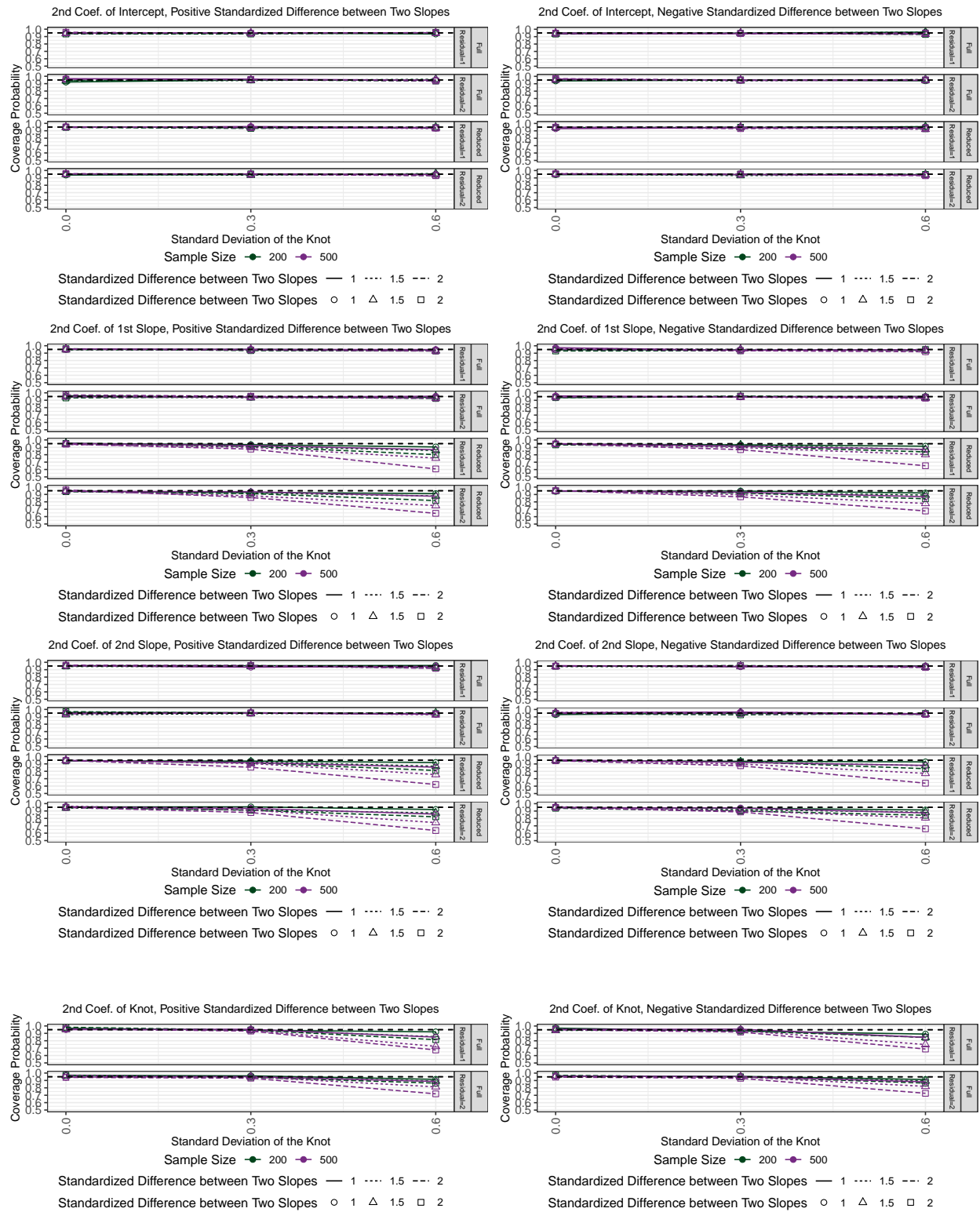


Figure B.8: Coverage Probability of Path Coefficients of x_2 in BLSGMs-TICs in the ITPs Framework (Under Conditions with 10 Repeated Measures, Midway Knot, Small Residuals and 13% Variances Explained by TICs)

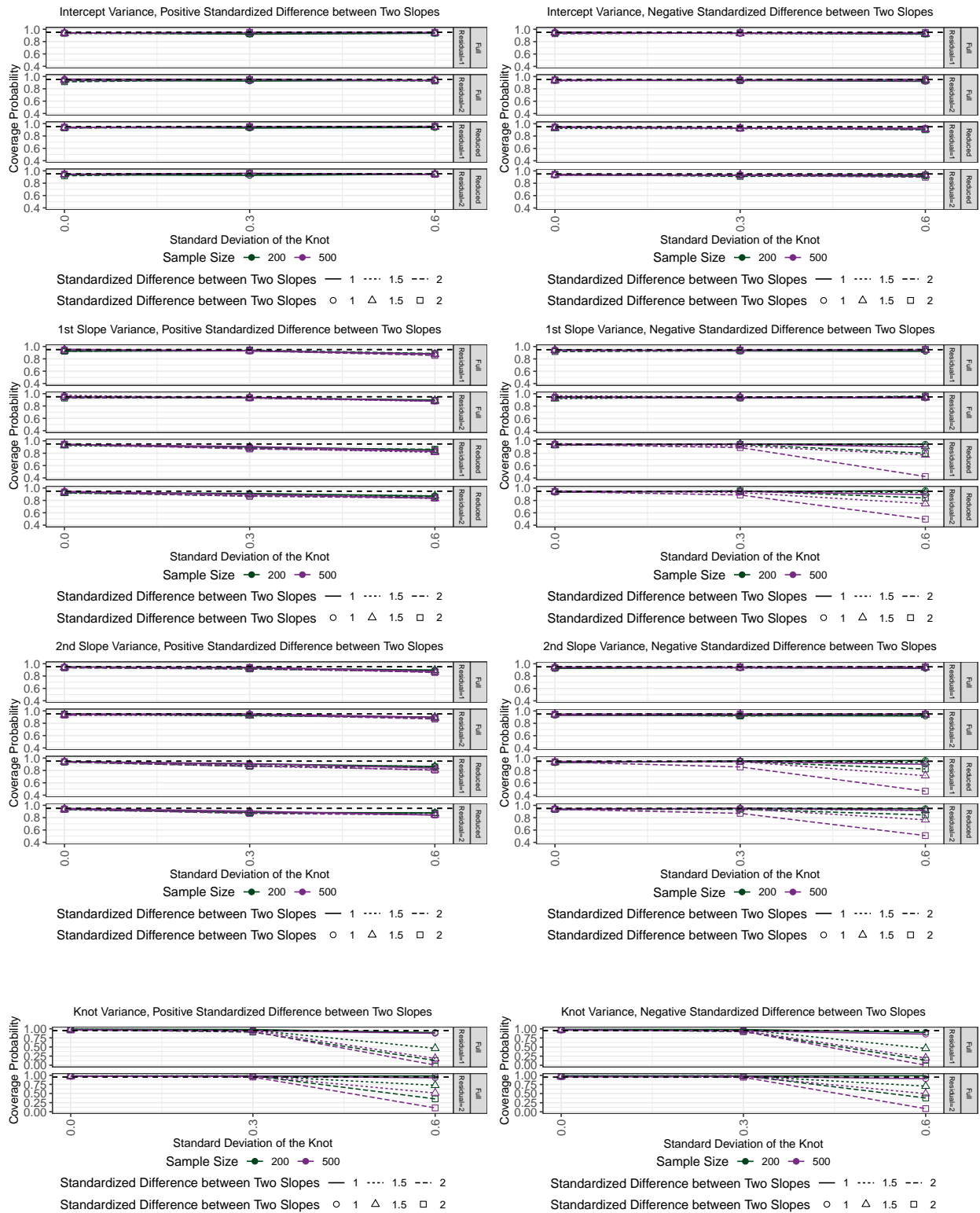


Figure B.9: Coverage Probability of Variances of Latent Variables in BLSGMs-TICs in the ITPs Framework (Under Conditions with 10 Repeated Measures Midway Knot and 13% Explained Variance)

Table 1: Simulation Design for BLSGM-TICs with an Unknown Knot in the ITPs Framework

Fixed Conditions	
Variables	Conditions
Mean of the Intercept	$\mu_{\eta_0} = 100$
Variance of the Intercept	$\psi_{00} = 25$
Mean of the 1st Slope	$\mu_{\eta_1} = -5$
Variance of Slopes	$\psi_{11} = \psi_{22} = 1$
Correlations of Growth Factors	$\rho = 0.3$
Manipulated Conditions	
Partially Crossed Design	
Variables	Conditions
Time (t_j)	6 scaled and equally spaced ($j = 0 \dots, J - 1, J = 6$) 10 scaled and equally spaced ($j = 0, \dots, J - 1, J = 10$)
(Mean of) the knot	μ_γ at $t = 2.5$ for $J = 6$ μ_γ at $t = 3.5$ or 4.5 or 5.5 for $J = 10$
Individual t_{ij}	$t_{ij} \sim U(t_j - \Delta, t_j + \Delta)$ ($j = 0, \dots, J - 1; \Delta = 0.25$)
Sample Size	$n = 200$ $n = 500$
Full Factorial Design	
Variables	Conditions
Standardized Difference d_z	$\mu_{\eta_1} - \mu_{\eta_2} = \pm 1.6$ (1.0-unit Standardized Difference) $\mu_{\eta_1} - \mu_{\eta_2} = \pm 2.4$ (1.5-unit Standardized Difference) $\mu_{\eta_1} - \mu_{\eta_2} = \pm 3.2$ (2.0-unit Standardized Difference)
Variance of Knots	$\psi_{\gamma\gamma} = 0$ ($sd(\gamma)/(t_j - t_{j-1}) = 0$) $\psi_{\gamma\gamma} = 0.09$ ($sd(\gamma)/(t_j - t_{j-1}) = 0.3$) $\psi_{\gamma\gamma} = 0.36$ ($sd(\gamma)/(t_j - t_{j-1}) = 0.6$)
Coefficients (B)	TICs explain 13% variability of growth factors TICs explain 26% variability of growth factors
Residual Variance	$\theta_\epsilon = 1$ $\theta_\epsilon = 2$

Table 2: Number of Improper Solutions among 1,000 Replications of the BLSGM-TICs in the ITPs Framework
(Conditions with 10 Repeated Measures & Midway Knot, 13% Explained Variance)

		$\theta_\epsilon = 1$		$\theta_\epsilon = 2$		
		$n = 200$	$n = 500$	$n = 200$	$n = 500$	
Small d_z	Positive d_z	$sd(\gamma) = 0$	555//48 ¹	516//22	550//40	507//29
		$sd(\gamma) = 0.3$	117//35	7//11	278//48	168//21
		$sd(\gamma) = 0.6$	4//3	0//0	58//25	7//6
	Negative d_z	$sd(\gamma) = 0$	535//37	542//27	568//44	531//27
		$sd(\gamma) = 0.3$	106//49	24//14	279//59	134//39
		$sd(\gamma) = 0.6$	0//8	0//0	67//45	8//17
Medium d_z	Positive d_z	$sd(\gamma) = 0$	563//49	553//28	583//39	573//22
		$sd(\gamma) = 0.3$	17//14	1//0	141//27	40//11
		$sd(\gamma) = 0.6$	0//1	0//0	9//2	0//0
	Negative d_z	$sd(\gamma) = 0$	568//42	542//26	576//50	513//32
		$sd(\gamma) = 0.3$	19//17	1//0	130//64	22//32
		$sd(\gamma) = 0.6$	0//0	0//0	4//23	0//0
Large d_z	Positive d_z	$sd(\gamma) = 0$	555//44	555//36	562//45	557//19
		$sd(\gamma) = 0.3$	1//0	0//0	27//19	0//0
		$sd(\gamma) = 0.6$	0//0	0//0	0//0	0//0
	Negative d_z	$sd(\gamma) = 0$	548//35	514//30	555//36	523//33
		$sd(\gamma) = 0.3$	1//2	0//0	37//39	2//6
		$sd(\gamma) = 0.6$	0//0	0//0	0//2	0//0

¹ 555//48 indicates that among 1,000 convergent replications of the BLSGM-TICs, we have 555 and 48 improper solutions due to negative knot variances and out-of-range correlations of the knot with other growth factors, respectively.

Table 3: Median (Range) of the Bias of Each Parameter in BLSGMs-TICs in the ITPs Framework of All Conditions

	Para.	Reduced BLSGM-TICs	Full BLSGM-TICs
		Median (Range)	Median (Range)
Mean Vector	μ_{η_0}	0.0004(-0.0858, 0.0821)	-0.0001(-0.0708, 0.0647)
	μ_{η_1}	0.0000(-0.1210, 0.1201)	0.0000(-0.1198, 0.1210)
	μ_{η_2}	0.0002(-0.1221, 0.1234)	0.0002(-0.1196, 0.1230)
	μ_{γ}	-0.0001(-0.0540, 0.0510)	0.0000(-0.0250, 0.0287)
Path Coef. of x_1	β_{10}	0.0014(-0.1132, 0.1025)	0.0008(-0.0472, 0.0378)
	β_{11}	0.0000(-0.1180, 0.1212)	0.0000(-0.0669, 0.0716)
	β_{12}	-0.0001(-0.1229, 0.1200)	-0.0001(-0.0634, 0.0620)
	$\beta_{1\gamma}$	-0.0641(-0.1502, 0.0000)	-0.0120(-0.1037, 0.0035)
Path Coef. of x_2	β_{20}	0.0002(-0.1352, 0.1366)	0.0004(-0.0460, 0.0597)
	β_{21}	0.0000(-0.1781, 0.1775)	-0.0001(-0.1029, 0.0997)
	β_{22}	0.0002(-0.1803, 0.1774)	0.0002(-0.1066, 0.0962)
	$\beta_{2\gamma}$	-0.0961(-0.2253, 0.0000)	-0.0185(-0.1565, 0.0033)
Unexplained Variance	ψ_{00}	-0.2229(-0.9849, 0.5176)	-0.2138(-0.6344, 0.0391)
	ψ_{11}	-0.0060(-0.0816, 0.3006)	-0.0088(-0.0737, 0.1457)
	ψ_{22}	-0.0066(-0.0873, 0.2978)	-0.0084(-0.0825, 0.1374)
	$\psi_{\gamma\gamma}$	-0.0724(-0.3132, 0.0000)	0.0017(-0.2041, 0.1033)

Table 4: Median (Range) of the RMSE of Each Parameter in BLSGMs-TICs in the ITPs Framework of All Conditions

	Para.	Reduced BLSGM-TICs	Full BLSGM-TICs
		Median (Range)	Median (Range)
Mean Vector	μ_{η_0}	0.2618(0.1850, 0.3665)	0.2620(0.1853, 0.3632)
	μ_{η_1}	0.0665(0.0387, 0.1547)	0.0668(0.0386, 0.1552)
	μ_{η_2}	0.0668(0.0382, 0.1594)	0.0670(0.0382, 0.1585)
	μ_{γ}	0.0471(0.0166, 0.1085)	0.0455(0.0168, 0.1082)
Path Coef. of x_1	β_{10}	0.2700(0.1969, 0.3811)	0.2692(0.1967, 0.3769)
	β_{11}	0.0711(0.0411, 0.1516)	0.0670(0.0412, 0.1254)
	β_{12}	0.0714(0.0410, 0.1517)	0.0670(0.0410, 0.1262)
	$\beta_{1\gamma}$	0.0641(0.0000, 0.1502)	0.0488(0.0119, 0.1450)
Path Coef. of x_2	β_{20}	0.2824(0.1979, 0.3851)	0.2768(0.1981, 0.3823)
	β_{21}	0.0752(0.0395, 0.2023)	0.0688(0.0398, 0.1533)
	β_{22}	0.0758(0.0401, 0.1996)	0.0683(0.0405, 0.1529)
	$\beta_{2\gamma}$	0.0961(0.0000, 0.2253)	0.0542(0.0115, 0.1928)
Unexplained Variances	ψ_{00}	1.7210(1.1470, 2.4947)	1.6779(1.1541, 2.4676)
	ψ_{11}	0.0883(0.0484, 0.3407)	0.0874(0.0491, 0.2619)
	ψ_{22}	0.0875(0.0472, 0.3374)	0.0876(0.0478, 0.2532)
	$\psi_{\gamma\gamma}$	0.0724(0.0000, 0.3132)	0.0646(0.0068, 0.2816)

Table 5: Summary of Model Fit Information For the Models

Latent Growth Curve Models						
Model	-2loglikelihood	AIC	BIC	# of Para.	Residual	
Linear	27298	27310	27334	6	75.60	
Quadratic	25320	25340	25379	10	35.14	
Jenss-Bayley	25330	25352	25396	11	35.37	
BLSGM (Fixed Knot)	25412	25434	25477	11	36.84	
BLSGM (Random Knot)	25308	25338	25398	15	33.06	
Latent Growth Curve Models with TICs						
Model	-2loglikelihood	AIC	BIC	# of Para.	Residual	
BLSGM-TICs (Random Knot)	31677	31809	32073	66	33.00	

Table 6: Estimates of the Proposed BLSGM-TICs

Growth Factor Parameter	Intercept			First Slope		
	Estimate	SE	P value	Estimate	SE	P value
Mean	26.859	0.588	< 0.0001*	1.731	0.018	< 0.0001*
Unexplained Variance	106.223	9.805	< 0.0001*	0.082	0.010	< 0.0001*
Sex (0–Boy; 1–Girl)	0.349	0.591	0.5548	−0.040	0.019	0.0353*
Race (0–White; 1–Other)	−0.432	0.597	0.4693	0.032	0.019	0.0921
School Location	−0.578	0.609	0.3426	−0.023	0.019	0.2261
Income	1.784	0.801	0.0259*	0.057	0.025	0.0226*
School Type (0–Public; 1–Private)	1.875	0.605	0.0019*	−0.028	0.019	0.1406
Parents' Highest Education	2.870	0.782	0.0002*	0.046	0.024	0.0553
Growth Factor Parameter	Second Slope			Knot		
	Estimate	SE	P value	Estimate	SE	P value
Mean	0.689	0.017	< 0.0001*	101.737	0.523	< 0.0001*
Unexplained Variance	0.014	0.008	0.0801	42.537	8.086	< 0.0001*
Sex (0–Boy; 1–Girl)	0.020	0.017	0.2394	−0.828	0.523	0.1134
Race (0–White; 1–Other)	−0.028	0.017	0.0995	−0.248	0.536	0.6436
School Location	−0.016	0.017	0.3466	1.612	0.539	0.0028*
Income	0.019	0.023	0.4088	−0.606	0.676	0.3700
School Type (0–Public; 1–Private)	−0.026	0.018	0.1486	0.114	0.529	0.8294
Parents' Highest Education	−0.023	0.022	0.2958	0.300	0.658	0.6484

* indicates statistical significance at 0.05 level.